Effect of the vector dose in *ip* administration

As *ip* administration appeared to be more promising than *iv*, we focused on the utility of *ip* in neonates. For this purpose, increasing doses of AAV5-CMV-hFIX vectors were tested. Higher hFIX concentrations were observed in animals with higher vector doses (Figure 1B). In the group with the highest vector dose (3×10^{11} genome copies/body weight (g.c./g)), the plasma hFIX concentrations were approximately 100 ng/ml, which is a therapeutically relevant level for severe hemophilia B, and these concentrations were sustained throughout the observation period.

Tissue distribution of the AAV vector genome

The tissue distribution of the vector genome after the *ip* injection into male mice was analyzed by real-time PCR. Substantial numbers of vector genomes were detected in the peritoneum and to a lesser extent in the liver and other tissues (Figure 1C). Note that the vector genomes are shown on a logarithmic scale.

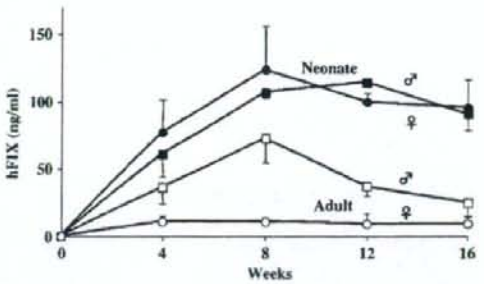

Figure 2. Plasma hFIX concentrations in mice after *ip* injections into different groups. The AAV5-CMV-hFIX vector at a dose of 3×10^{11} g.c./g was injected into C57BL/6 neonatal males (n = 6, closed squares), neonatal females (n = 4, closed circles), adult males (n = 4, open squares), and adult females (n = 4, open circles)

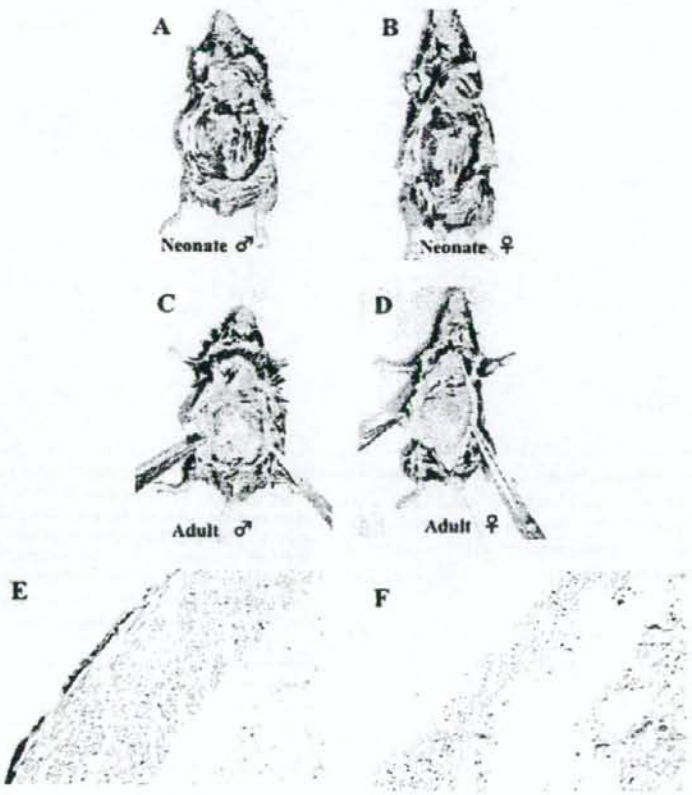

Figure 3. β-Galactosidase expression at 8 weeks after *ip* injection of the AAV5-CMV-LacZ vector at a dose of 1×10^{11} g.c./g in the C57BL/6 mice (A–D). X-gal staining was performed after removal of the intraperitoneal organs. Histochemistry with β-galactosidase performed on tissues from the neonatal male peritoneum after the injection stained the mesothelium (E) and the untransduced control (F) (final magnification ×100)

DOI: 10.1002/jgm

Influence of sex and age of mice on transgene expression

In order to compare the efficiency with regard to the sex and age of mice during administration, the same dose of the AAV vector based on the body weight (3×10^{11} g.c./g) was administered by *ip* injection to both neonatal and adult mice. As summarized in Figure 2, the plasma levels of hFIX were significantly higher in males than in females when adults were used ($p < 0.05$). On the other hand, there were no sex-related differences in the hFIX concentration in neonates. Moreover, the hFIX levels were much higher in neonates (neonate vs. adult; $p < 0.05$ in males, $p < 0.01$ in females). After 8 weeks, a considerable reduction in the plasma hFIX concentration was observed in adult males.

Tissue distribution of transgene expression following *ip* injection

To evaluate the efficacy and location of transgene expression following *ip* vector administration, 1×10^{11} g.c./g of the AAV5-CMV-LacZ vector was injected into either neonatal or adult mice. After 8 weeks, the mice were sacrificed and their tissues were subjected to X-gal staining. As shown in Figures 3A–3D, β-galactosidase expression was observed in the peritoneum. Robust β-galactosidase expression was observed in both male and female mice in the neonatal group (Figures 3A and 3B). In contrast, in the injected adults, only weak β-galactosidase expression was observed in the male mice, and faint expression was detected in the female mice (Figures 3C and 3D). Other tissues were also analyzed by X-gal staining, and none of these, including liver and kidney, showed positive results (data not shown). Microscopic examination of the peritoneum of neonatally injected male mice revealed β-galactosidase expression in mesothelial cells, while the control mice did not show X-gal positivity (Figures 4E and 4F).

In vivo and *ex vivo* analysis using bioluminescence

To quantify the distribution of transgene expression, the AAV5-CMV-Luc vectors were administered *ip* to neonatal and adult mice at an equivalent vector dose based on the body weight (3×10^9 g.c./g). Luciferase expression was observed by *in vivo* bioluminescence imaging 10 weeks after the vector injection (Figures 4A–4D). Quantitative results of *in vivo* bioluminescence are shown in Figure 4E. In neonates, no sex-related difference was found in luciferase expression ($3.8 \times 10^9 \pm 1.2 \times 10^8$ photons/s and $2.9 \times 10^9 \pm 1.0 \times 10^9$ photons/s for the males and females, respectively, $p = 0.13$). In contrast, a significant difference in distribution and quantitation was observed in adults ($1.3 \times 10^9 \pm 7.2 \times 10^8$ photons/s and $5.3 \times 10^7 \pm 1.6 \times 10^7$ photons/s for males and females, respectively, $p < 0.05$). In order to identify the tissues responsible for luciferase expression, an *ex vivo* bioluminescence analysis was performed at 10 weeks after the vector injection; this demonstrated that the luciferase expression was localized in the peritoneum (Figure 5A). As shown on the pseudocolor scale, the white color showed background of the assay and did not reflect luciferase expression. A luminometric analysis of individual tissues from representative animals revealed a difference in the expression in the peritoneum among the injected neonates and adults (3.1×10^8 and 1.6×10^8 photons/s/g for male and female neonates, respectively; 1.1×10^8 and 7.9×10^4 photons/s/g for male and female adults, respectively) (Figure 5B).

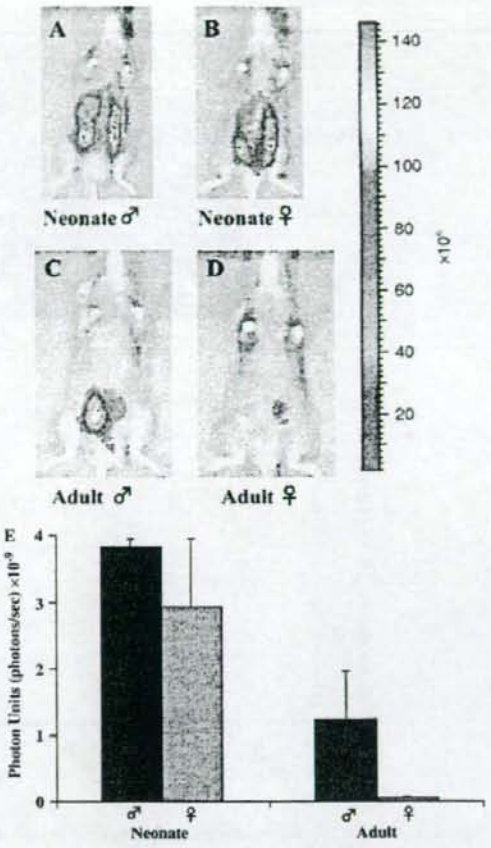

Figure 4. ***In vivo*** **bioluminescence imaging at 10 weeks after *ip* injection of the AAV5-CMV-Luc vector at a dose of 5×10^9 g.c./1.5 g in the C57BL/6 mice (A–D). Images were analyzed under the same condition, and the reference color bar, indicating the photon units (photons/s), is the same for all mice. (E) Quantitative results of *in vivo* bioluminescence imaging in neonatal males (n = 6, closed columns) and females (n = 4, hatched column), and adult males (n = 5, dotted column) and females (n = 5, open column), are shown. Mice were transduced with 5×10^9 g.c./1.5 g of the AAV5-CMV-Luc vector (2.5×10^8 g.c./μl). The ordinate indicates the photon units (photon/s)**

DOI: 10.1002/jgm

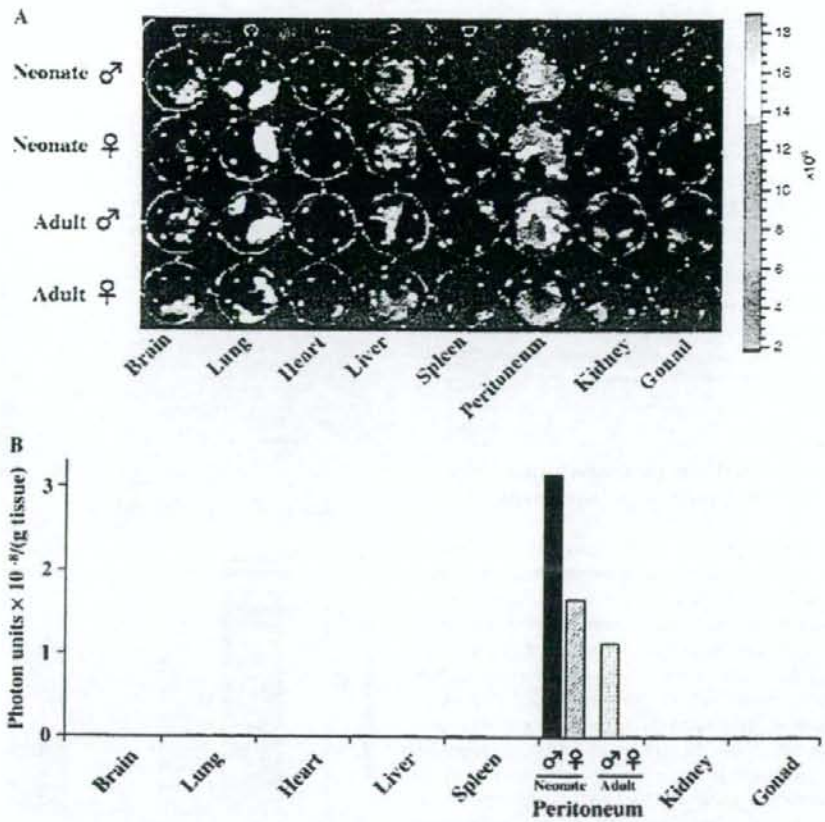

Figure 5. Analysis of tissue-specific expression after *ip* injection of the AAV5-CMV-Luc vector. (A) *Ex vivo* bioluminescence images of injected neonates and adults are shown. Mice were sacrificed at 10 weeks after vector injection and the major organs were extracted and placed into each well of a 24-well dish containing luciferin substrate solution in order to measure the individual bioluminescence. (B) Quantitative results of transgene expression are as indicated in (A). The ordinate shows the photon units (photons/s)

Discussion

In this study, we tested the utility of neonatal gene transfer by using AAV5-based vectors. All genes tested – *lacZ*, *hfIX*, and *luc* – demonstrated robust transgene expression after *ip* injection. The advantage of neonatal gene transfer was clearly demonstrated by the plasma hFIX levels after injecting both adult and neonatal mice with equivalent doses of the AAV-CMV-hFIX vector (3×10^{11} g.c./g). Throughout the observation period, a higher hFIX concentration was detected in neonates than in adults; therapeutic levels of hFIX were maintained even after maturation (Figure 2). Another comparison using vectors encoding luciferase at an equivalent vector dose also resulted in a higher transgene expression in neonates (Figure 4). These data support the advantages of neonatal gene transfer.

Neonatal gene delivery in mice is technically difficult due to their size. In this study, we demonstrated the usefulness of *ip* injections as a route of vector delivery. On the other hand, we did not include the *im* route in this series of experiments because the injection volume was strictly limited in neonates. However, this latter method is apparently an attractive route of administration in clinical applications. Therefore, the efficacy of *im* administration requires further analysis in larger animal models.

In this study, transgene expression was mostly confined to the peritoneum after *ip* injection into neonates. This was confirmed by different modes of detection. In addition, the vector genome distribution was mostly comparable to the level of transgene expression. However, in a previous report, transgene expression was also observed in tissues other than the peritoneum when fetuses were injected [17]. Since the vector system and the promoter were the same, the difference in tissue distribution may be related to the age at the time of injection, vector dose, technical details, or other unrecognized factors. At present, the mechanism responsible for tissue specificity is not clear. The abundance of receptor molecules, such as platelet-derived

DOI: 10.1002/jgm

growth factor (PDGF) receptors [27], may contribute to this phenomenon. Using other vector systems may result in different tissue specificity. Recently, transgene expression in the whole peritoneal cavity was observed by *ip* administration of polyethylenimine (PEI)/DNA complexes [28]. Further, in neonates, a long-term expression was observed in factor IX concentration, whereas in adult males a sharp decrease was observed at 12 weeks and later (Figure 3). When the peritoneum was analyzed, only the surface epithelium of the peritoneal tissue was transduced (Figure 4E), and it appeared to be responsible for continuously supplying the transgene product at a therapeutic level. These cells contain an extremely high copy number of transgenes even after a prolonged period of time (Figure 2C). The copy number of the vector genome within the peritoneum appears to be underestimated thus far because the whole peritoneal tissue was used for DNA extraction prior to Q-PCR. The presence of an extremely high copy number of vector genomes within the peritoneum is possibly related to the robust and persistent transgene expression in neonatal gene transfer. The mechanism for the persistence of high copy number and transgene expression is interesting and may offer important insights into the biology of the AAV vector.

Interestingly, a sex-related difference in transgene expression within the peritoneal tissues was observed after *ip* injection into adult mice regardless of the transgene. In a previous study, a sex-related difference in transgene expression was demonstrated in the liver, and an androgen-dependent pathway appeared to be involved [25,26]. We have also demonstrated an overwhelming sex-related difference in liver transduction efficiency in a mouse model [19]. Based on our knowledge, this is the first report that demonstrates a sex-related difference in transgene expression in tissues other than the liver. At present, it is not clear whether the same mechanism is involved in the peritoneal tissue. The difference may be a drawback when an attempt is made to transfer genes into females. However, our results indicate that this problem can be circumvented if neonates are targeted for gene therapy.

Neonatal gene transfer is also advantageous from an immunological point of view. Due to the immaturity of the neonatal immune system, tolerance to an 'immunogenic' transgene product can be induced. Recently, neonatal and fetal gene transfer experiments using adenoviral and retroviral vectors demonstrated the induction of tolerance to transgene products [14,15]. In our series of experiments, it is difficult to prove this point because all transgenes were expressed for a long period even in adults. Nonetheless, divergent levels of transgene expression between adults and neonates may reflect a difference in immunology, and needs to be analyzed in the future.

In conclusion, our findings support the efficacy of neonatal gene therapy and would help to design strategies for neonatal gene therapy using AAV vectors.

Acknowledgements

We thank Dr. Y. Hakamata (Animal Resource Project, Jichi Medical School) for providing technical assistance in the animal experiments. This work was partly supported by grants from the Ministry of Education, Culture, Sports, Science and Technology, and the Ministry of Health, Labor and Welfare, Japan; the 'High-Technology Research Center' Project for Private Universities: a matching fund subsidy from the Ministry of Education, Culture, Sports, Science and Technology, 2003–2007; and the 21st Century Centers of Excellence Program from the Ministry of Education, Culture, Sports, Science and Technology.

References

1. Chao H, Samulski R, Bellinger D, *et al.* Persistent expression of canine factor IX in hemophilia B canines. *Gene Ther* 1999; **6**: 1695–1704.
2. Herzog RW, Yang EY, Couto LB, *et al.* Long-term correction of canine hemophilia B by gene transfer of blood coagulation factor IX mediated by adeno-associated viral vector. *Nat Med* 1999; **5**: 56–63.
3. Mount JD, Herzog RW, Tillson DM, *et al.* Sustained phenotypic correction of hemophilia B dogs with a factor IX null mutation by liver-directed gene therapy. *Blood* 2002; **99**: 2670–2676.
4. Snyder RO, Miao C, Meuse L, *et al.* Correction of hemophilia B in canine and murine models using recombinant adeno-associated viral vectors. *Nat Med* 1999; **5**: 64–70.
5. Kay MA, Manno CS, Ragni MV, *et al.* Evidence for gene transfer and expression of factor IX in haemophilia B patients treated with an AAV vector. *Nat Genet* 2000; **24**: 257–261.
6. Manno CS, Chew AJ, Hutchison S, *et al.* AAV-mediated factor IX gene transfer to skeletal muscle in patients with severe hemophilia B. *Blood* 2003; **101**: 2963–2972.
7. Arruda VR, Schuettrumpf J, Herzog RW, *et al.* Safety and efficacy of factor IX gene transfer to skeletal muscle in murine and canine hemophilia B models by adeno-associated viral vector serotype 1. *Blood* 2004; **103**: 85–92.
8. Chao H, Liu Y, Rabinowitz J, *et al.* Several log increase in therapeutic transgene delivery by distinct adeno-associated viral serotype vectors. *Mol Ther* 2000; **2**: 619–623.
9. Chao H, Monahan PE, Liu Y, Samulski RJ, Walsh CE. Sustained and complete phenotype correction of hemophilia B mice following intramuscular injection of AAV1 serotype vectors. *Mol Ther* 2001; **4**: 217–222.
10. Mingozzi F, Schuettrumpf J, Arruda VR, *et al.* Improved hepatic gene transfer by using an adeno-associated virus serotype 5 vector. *J Virol* 2002; **76**: 10 497–10 502.
11. Coutelle C, Themis M, Waddington S, *et al.* The hopes and fears of in utero gene therapy for genetic disease–a review. *Placenta* 2003; **24**(Suppl B): S114–121.
12. Mitchell M, Jerebtsova M, Batshaw ML, Newman K, Ye X. Long-term gene transfer to mouse fetuses with recombinant adenovirus and adeno-associated virus (AAV) vectors. *Gene Ther* 2000; **7**: 1986–1992.
13. Themis M, Schneider H, Kiserud T, *et al.* Successful expression of beta-galactosidase and factor IX transgenes in fetal and neonatal sheep after ultrasound-guided percutaneous adenovirus vector administration into the umbilical vein. *Gene Ther* 1999; **6**: 1239–1248.
14. Waddington SN, Buckley SM, Nivsarkar M, *et al.* In utero gene transfer of human factor IX to fetal mice can induce postnatal tolerance of the exogenous clotting factor. *Blood* 2003; **101**: 1359–1366.
15. Zhang J, Xu L, Haskins ME, Parker Ponder K. Neonatal gene transfer with a retroviral vector results in tolerance to human factor IX in mice and dogs. *Blood* 2004; **103**: 143–151.
16. Schneider H, Muhle C, Douar AM, *et al.* Sustained delivery of therapeutic concentrations of human clotting factor IX–a comparison of adenoviral and AAV vectors administered in utero. *J Gene Med* 2002; **4**: 46–53.
17. Lipshutz GS, Titre D, Brindle M, *et al.* Comparison of gene expression after intraperitoneal delivery of AAV2 or AAV5 in utero. *Mol Ther* 2003; **8**: 90–98.

18. Mochizuki S, Mizukami H, Kume A, *et al.* Adeno-associated virus (AAV) vector-mediated liver- and muscle-directed transgene expression using various kinds of promoters and serotypes. *Gene Ther Mol Biol* 2004; **8**: 9–18.
19. Mochizuki S, Mizukami H, Ogura T, *et al.* Long-term correction of hyperphenylalaninemia by AAV-mediated gene transfer leads to behavioral recovery in phenylketonuria mice. *Gene Ther* 2004; **11**: 1081–1086.
20. Herzog RW, Hagstrom JN, Kung SH, *et al.* Stable gene transfer and expression of human blood coagulation factor IX after intramuscular injection of recombinant adeno-associated virus. *Proc Natl Acad Sci U S A* 1997; **94**: 5804–5809.
21. Mimuro J, Mizukami H, Ono F, *et al.* Specific detection of human coagulation factor IX in cynomolgus macaques. *J Thromb Haemost* 2004; **2**: 275–280.
22. Matsushita T, Elliger S, Elliger C, *et al.* Adeno-associated virus vectors can be efficiently produced without helper virus. *Gene Ther* 1998; **5**: 938–945.
23. Grimm D, Zhou S, Nakai H, *et al.* Preclinical in vivo evaluation of pseudotyped adeno-associated virus vectors for liver gene therapy. *Blood* 2003; **102**: 2412–2419.
24. Kanazawa T, Mizukami H, Okada T, *et al.* Suicide gene therapy using AAV-HSVtk/ganciclovir in combination with irradiation results in regression of human head and neck cancer xenografts in nude mice. *Gene Ther* 2003; **10**: 51–58.
25. Davidoff AM, Ng CY, Zhou J, Spence Y, Nathwani AC. Sex significantly influences transduction of murine liver by recombinant adeno-associated viral vectors through an androgen-dependent pathway. *Blood* 2003; **102**: 480–488.
26. Nathwani AC, Davidoff A, Hanawa H, *et al.* Factors influencing in vivo transduction by recombinant adeno- associated viral vectors expressing the human factor IX cDNA. *Blood* 2001; **97**: 1258–1265.
27. Di Pasquale G, Davidson BL, Stein CS, *et al.* Identification of PDGFR as a receptor for AAV-5 transduction. *Nat Med* 2003; **9**: 1306–1312.
28. Louis M-H, Dutoit S, Denoux Y, *et al.* Intraperitoneal linear polyethylenimine (L-PEI)-mediated gene delivery to ovarian carcinoma nodes in mice. *Cancer Gene Ther* 2006; **13**: 367–374.

Prevention of diabetic retinopathy by intraocular soluble *flt-1* gene transfer in a spontaneously diabetic rat model

JUNICHI IDENO[1,2], HIROAKI MIZUKAMI[1], AKIHIRO KAKEHASHI[3], YUKA SAITO[3], TAKASHI OKADA[1], MASASHI URABE[1], AKIHIRO KUME[1], MASATOSHI KUROKI[4], MASANOBU KAWAKAMI[4], SHUN ISHIBASHI[2] and KEIYA OZAWA[1]

[1]Division of Genetic Therapeutics, Center for Molecular Medicine, [2]Department of Medicine, Division of Endocrinology and Metabolism, Jichi Medical University, Tochigi, Japan; [3]Department of Ophthalmology, [4]Department of Comprehensive Medicine I, Omiya Medical Center, Jichi Medical University, Saitama, Japan

Received August 11, 2006; Accepted October 2, 2006

Abstract. The number of patients suffering from diabetes mellitus is constantly rising worldwide, and diabetic retinopathy (DR) has become the most frequent cause of postnatal blindness. Vascular endothelial growth factor (VEGF) is known to play a central role during DR development. Thus, inhibiting the effects of VEGF may hamper the disease progression, and gene transfer of the soluble VEGF receptor *sflt-1* is an attractive approach for this purpose. However, the lack of suitable animal models hindered the evaluation of this strategy. Recently, the spontaneously diabetic non-obese Torii (SDT) rat was established and is considered as one of the ideal models for human DR. In this study, we evaluated the efficacy of gene therapy in SDT rats by using adeno-associated viral vectors (AAV-*sflt-1*) injected into the subretinal space. Thirty weeks later, the progression of DR was assessed by fluorescein angiography using three parameters; the presence of an avascular area, extensive hyperfluorescein and arterial narrowing. These changes were significantly less evident in the 'treated' eyes than in the control. No adverse effects were observed throughout the study. These results indicate that local *sflt-1* gene transfer inhibits DR progression in SDT rats and offers powerful therapeutic potential for the management of human DR.

Introduction

Diabetic retinopathy (DR) is one of the major complications of diabetes mellitus (DM), and the most frequent cause of postnatal blindness (1,2). The number of patients suffering from DM is steadily increasing worldwide (3), and the prevention of DR has become a matter of great importance. Unfortunately, the number of patients who are losing their vision due to DR is increasing despite the technological advancements, especially laser photocoagulation and vitreous surgery. Therefore, the development of a novel therapeutic approach to prevent DR progression has a vital significance.

Proliferative diabetic retinopathy (PDR) is an advanced form of DR characterized by neovascularization, vitreous hemorrhage and tractional retinal detachment. Although a number of biochemical changes, including increased polyol pathway activity (4,5), activation of protein kinase C (6-8) and accumulation of advanced glycation end-products (9,10) were reported in the development of PDR, vascular endothelial growth factor (VEGF), a potent endothelial cell-specific mitogen, plays a critical role in the angiogenesis of PDR (11-13). The actions of VEGF are mediated by the fms-like receptors, Flt-1 and Flk-1/KDR, which are expressed on vascular endothelial cells, and result in endothelial cell proliferation, migration, and increased vasopermeability with tyrosine kinase activity (14-17). Expression of VEGF is upregulated by hypoxia, and increased vitreous VEGF levels were observed in patients with PDR (12,18,19). Moreover, overexpression of VEGF by photo-receptors in transgenic mice promoted retinal neovascular-ization (20), whereas antagonists for VEGF suppressed neovascularization in the retina and iris (13,21,22). A soluble form of the VEGF receptor Flt-1 (sFlt-1) is the only known endogenous specific inhibitor for VEGF, and has drawn considerable attention for its potential clinical application in the inhibition of angiogenesis (23-28). It lacks the immuno-globulin-like domain, the transmembrane spanning region and the intracellular tyrosine-kinase domain. The anti-angiogenic activity of sFlt-1 results from the inhibition of VEGF by two mechanisms; the sequestration of VEGF and the formation of inactive heterodimers with membrane spanning isoforms of the VEGF receptors Flt-1 and KDR (26,29). Studies have shown that the administration of viral vectors encoding *sflt-1* inhibited retinal neovascularization in animal models (30,31). However, the actual merits of sFlt-1 in clinically relevant DR models have not been evaluated.

Correspondence to: Dr Hiroaki Mizukami, Division of Genetic Therapeutics, Center for Molecular Medicine, Jichi Medical University, 3311-1 Yakushiji, Shimotsuke, Tochigi 329-0498, Japan
E-mail: miz@jichi.ac.jp

Key words: diabetic retinopathy, gene therapy, *sflt-1*, spontaneously diabetic non-obese Torii rat, adeno-associated viral vector

Recently, a spontaneously diabetic, non-obese Torii (SDT) rat strain was established from the Sprague-Dawley lineage (32). The animals develop DM at ~20 weeks of age and later manifest DR, which is characterized by tractional retinal detachment, retinal hemorrhage, extensive venous dilatation, extensive hyperfluorescence and a non-perfusion area beyond 55 weeks of age (33). These findings are similar to those found in DR patients; therefore, the SDT rat is one of the best-suited models for studying human DR.

Adeno-associated viral (AAV) vectors are becoming popular in the field of gene therapy because of their safety and long-term effectiveness (34,35). A number of studies have demonstrated the efficacy of ocular gene therapy using AAV vectors (30,36), and vectors derived from serotype 5 (rAAV5) showed the highest utility for retinal gene transfer among serotypes tested (37-39). For this reason, we set out to test the utility of gene therapy on preventing DR in SDT rats using an rAAV5 vector encoding human *sflt-1* (rAAV5-*sflt-1*).

Materials and methods

rAAV vector construction and production. The *sflt-1* cDNA was amplified by PCR from the cDNA library of human umbilical vein endothelial cells (HUVEC). The *in vitro* effect of *sflt-1* expression was confirmed according to a method previously reported (40,41). Briefly, a plasmid was transfected into 293 cells with the Ca-phosphate method, the medium from 293 cells was added at specified dilutions to a 96-well plate containing HUVEC, and the cell density was assessed. An rAAV5 vector encoding *sflt-1* cDNA driven by the human cytomegalovirus (CMV) promoter (rAAV5-CMV-*sflt-1*) was constructed (Fig. 1). rAAV vectors were produced with an adenovirus-free system, and were purified by ultracentrifugation through an Iodixanol (Axis-Shield PoC AS, Oslo, Norway) gradient followed by dialysis (42,43). The titers of the vector stocks were determined by quantitative dot-blot analysis using a BAS-1500 image analyzer (Fuji Film, Tokyo, Japan).

Animals. All animal experiments were performed in accordance with the standards in the Guide for the Care and Use of Laboratory Animals (NIH publication no. 85-23) and the institutional guidelines. Male SDT rats, provided by the Association for the Spontaneously Diabetic Torii Rat, were used in this study. Standard rodent diet and water were provided *'ad libitum*. Casual blood glucose levels were measured by the glucose-oxydase method every four weeks using Glutest A (Sanwa Chemical, Tokyo, Japan). Glycosylated hemoglobin (HbA1c) was measured with a latex agglutination test (SRL, Tokyo, Japan), and plasma sFlt-1 levels were determined using a commercially available ELISA kit (Bender MedSystems, San Bruno, CA) at the end of the study.

Subretinal injection of vector solution. Rats at the age of 27 weeks were anesthetized with an intraperitoneal injection of pentobarbital sodium (1 mg/kg), and 0.4% oxybuprocaine chloride eye drops were used for additional analgesia. All surgical procedures were performed under a surgical microscope. The tip of a 10-mm 39-gauge nylon needle

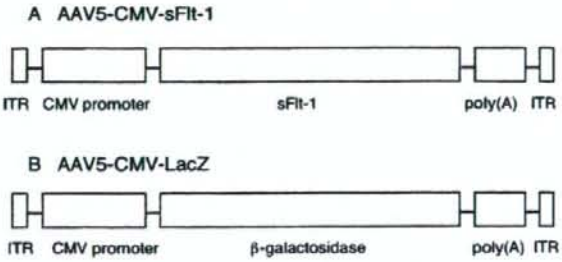

Figure 1. Structure of rAAV vectors. (A) rAAV5-CMV-*sflt-1* vector. (B) rAAV-CMV-*lacZ* vector. ITR, inverted terminal repeat of AAV serotype 5; CMV, human cytomegalovirus promoter; GH, human growth hormone first intron enhancer; Poly (A), SV40 early poly A.

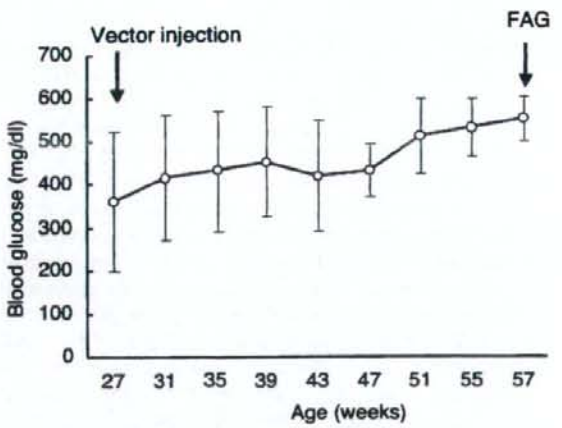

Figure 2. Blood glucose levels of animals during the study. All rats developed diabetes mellitus by the time of subretinal vector administration, and high glucose levels continued throughout the study. Data were shown as mean ± SD, (n=8). FAG, fluorescein angiography.

(Bausch & Lomb, Rochester, NY), mounted on a 10-μl Hamilton syringe, was inserted into the subretinal space through the sclera and ~10 μl of viral suspension was injected. Treated eyes received rAAV5-CMV-*sflt-1* ($4x10^{10}$ vector genome/eye) plus rAAV5 expressing ß-galactosidase (rAAV5-CMV-*lacZ*, $1x10^{10}$ vector genome/eye). Control eyes received only rAAV-CMV-*lacZ* ($1x10^{10}$ viral genome/eye).

Fluorescein-dextran microscopy and quantification of DR. Thirty weeks after the vector administration, the progression of DR was evaluated using fluorescein angiography (FAG). Cardiac perfusion was performed with 1 ml of PBS containing 50 mg of fluorescein-labeled dextran (fluorescein isothiocyanate-dextran; MW, $2x10^6$ daltons; Sigma, St Louis, MO), after administration of a lethal dose of pentobarbital sodium. The eyes were enucleated, the cornea and lens were removed, and the retina dissected from the eyecup. The retina was cut radially and flat-mounted on a glass slide without fixation. A drop of aqueous mounting medium (Crystal/mount, Biomeda

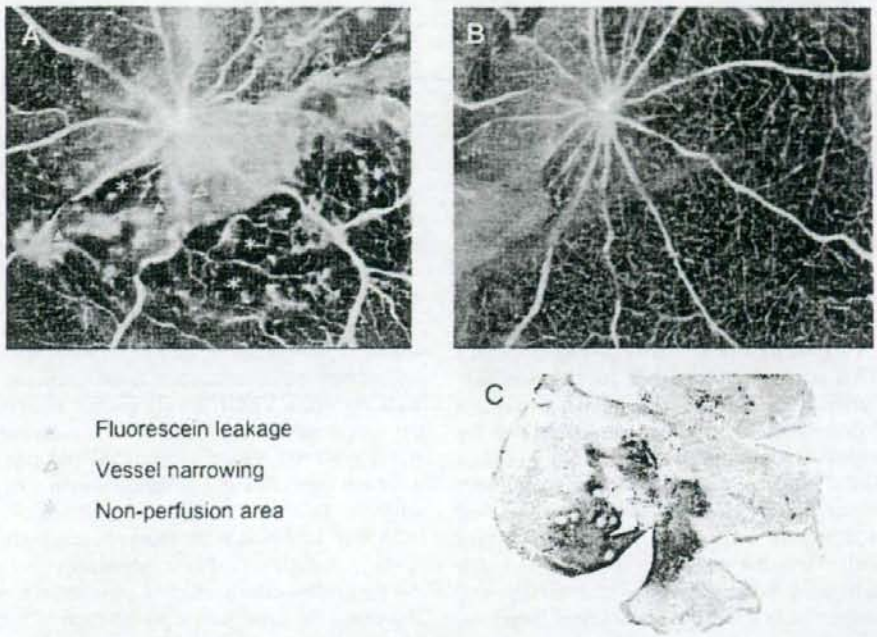

Figure 3. Fluorescein microangiography (FAG) of the rats 30 weeks after vector administration. (A) FAG from AAV5-CMV-*lacZ* injected rats. (B) FAG from rAAV5-CMV-*sflt-1* plus rAAV5-CMV-*lacZ* injected rats. The leakage from the fluorescein spot and avascular area are less extensive in B than in A, thus indicating that the progression of diabetic retinopathy is less marked in the rats treated with rAAV5-CMV-*sflt-1*. (C) A typical X-gal staining of the rat retina showing the distribution of the transduced tissue after subretinal injection of the rAAV-CMV-*lacZ* vector.

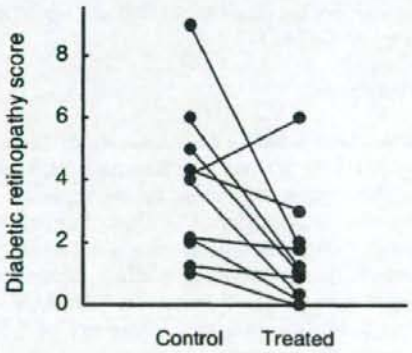

Figure 4. Diabetic retinopathy score of the rats evaluated at the end of the study. The Wilcoxon signed-ranks test demonstrates that the scores for the treated eyes are significantly less than those for the control eyes (n=8, $p<0.05$).

Corp, Foster City, CA) was applied over the retina and allowed to dry. Then the whole flat-mounted retina was examined by fluorescent microscopy (Nikon Labphoto, Nikon, Tokyo, Japan). Without providing information on the vectors injected, the status of DR was determined using the following three parameters: the presence of an avascular area, extensive hyperfluorescence, and arterial narrowing. Each parameter was scored from 0 (none) to 3 (severe) based upon the findings of FAG. The score for each eye was compared and analyzed using the Wilcoxon signed-ranks test. Rats that did not show DR in either of the eyes were excluded from the study. To confirm the subretinal injection of vector solution, X-gal staining of the eye was performed after FAG.

Results

Effect of sFlt-1 in vitro. To prove the biological activity of the protein produced from the *sflt-1* cDNA *in vitro*, we incubated HUVEC with different dilutions of media from 293 cells transfected with the plasmid. The conditioned media from transfected cells inhibited proliferation of HUVEC in a dose-dependent manner, whereas media from untransfected cells had no effect on HUVEC proliferation (data not shown).

Development of DM in SDT rats. All rats developed DM by 35 weeks of age and high blood glucose levels continued throughout the study (Fig. 2). At the end of the study, HbA1c levels in all rats were high (9.4±0.95%; means ± SD), and plasma sFlt-1 was not detected. No adverse effects of sFlt-1 gene therapy were observed throughout the study.

Evaluation of efficacy of gene transfer into the retina. Thirty weeks after the vector administration, FAG was performed to determine the progression of DR. DR was diagnosed using three parameters, arterial narrowing, pooling of fluorescein and a non-perfusion area, and the severity of these parameters were evaluated. The scores of DR in the treated eyes were significantly less than those in the control eyes (Fig. 3A and B; Fig. 4). X-gal staining demonstrated that the LacZ protein was produced in the retinal tissue after transduction with the

rAAV5 vector, and the transgene expression persisted for over 30 weeks after vector administration (Fig. 3C).

Discussion

VEGF is supposedly one of the most essential factors in retinal neovascularization during DR progression. The inhibition of retinal neovascularization by *sflt-1* gene transfer in animal models has been demonstrated in earlier reports (30,31). However, since the mechanisms underlying neovascularization in these models were not related to hyperglycemia, the effectiveness of sFlt-1 in inhibiting DR had not been estimated. To shed light on this issue, a more clinically relevant model has long been awaited. The recently developed SDT rat model is a candidate for this purpose. This model is unique because its diabetic status mimics human NIDDM rather than IDDM. The animals can live for 1 year after the onset of DM without insulin, with a gradual maturation of DR. Therefore, this model is a valuable tool because it can reflect mid- to late-stage human DR associated with NIDDM (32,33). However, this model has certain drawbacks as well. First, the disease progression is much slower than that in other 'conventional' animal models, and DR can be observed mainly after 55 weeks of age. Therefore, one series of experiments requires a long time period. Second, these animals are prone to death, probably due to the complications of DM. Unfortunately, the number of animals decreases before they develop sufficient disease severity. Therefore, to ensure valid results, the sample size of each group needs to be sufficiently large.

This study aimed to demonstrate the efficacy of gene therapy in preventing DR disease progression. For this purpose, we injected the vector soon after the onset of DM, and the efficacy was evaluated at the age of full-blown DR. Considering that a preventive action was significant in this study, a more precise examination of whether short-term *sflt-1* expression is sufficient to prevent DR progression or has an effect in reversing the DR status should be considered for future study. A more difficult task includes determining effective methods to develop this strategy into a clinically realized therapy. Generally, if the therapeutic efficacy is proven in small animals, additional experiments need to be performed on larger animals prior to conducting clinical trials. Regarding DR, no appropriate model has been found in species of large animals. Proliferative DR-like changes were observed in a galactose-fed dog model (44). Nevertheless, this model requires up to 7 years to establish mature DR, which is impractical in a preclinical study. Development of novel large animal models for this purpose is ideal but not practical due to the uncertainty of success in establishing such models during a defined time range. Resolving this problem may not be easy; however, we believe that before clinical trials are considered, further studies using large animals are essential.

In this study, the area of transgene expression was sufficiently wide to protect vision, and the expression continued for over 30 weeks after the injection, indicating that rAAV-mediated ocular gene transfer via a single injection of vector solution could lead to a long-term therapeutic effect. The area of *sflt-1* expression should be comparable to that of X-gal staining, although human sFlt-1 in the retina was undetectable by immunohistochemistry. This may have occurred probably due to technical difficulties in localizing the soluble antigen (31). Therefore, ocular gene transfer under the present experimental conditions is a practical approach. Nonetheless, DR progression was suppressed partially and not completely. At present, it is unclear whether the incomplete suppression was due to the residual actions of VEGF or the uninhibited activity of an alternative angiogenic factor (45). Regarding the latter, a combination of transgenes that act on different aspects of angiogenesis may increase the efficacy of gene therapy for DR prevention.

In patients with DM, VEGF is closely involved in the degree of complication. Elevated VEGF levels in the retina may worsen the DR status and cause visual loss (11,12), while high systemic VEGF levels induce neovascularization, improving ischemic conditions. If circulating sFlt-1 levels affect systemic VEGF levels, DM patients may develop ischemic heart disease, diabetic neuropathy, and diabetic gangrene. To avoid these adverse effects, local sFlt-1 delivery and VEGF inhibition is necessary. In this study, plasma sFlt-1 levels were not elevated after subretinal vector administration, and no adverse effects of *sflt-1* gene transfer were observed. Therefore, the subretinal administration of a vector solution and neutralization of the VEGF activity *in situ* appear to be appropriate measures that should be adopted to achieve our goal.

In conclusion, we demonstrated the successful prevention of DR in SDT rats by using an rAAV vector-encoding *sflt-1* gene. These findings strongly suggest the efficacy of sFlt-1 for DR and the usefulness of rAAV5 for ocular gene transfer. Further studies are necessary to develop and optimize ocular gene therapy for human DR.

Acknowledgements

We thank the Association for the Spontaneously Diabetic Torii Rat for providing the SDT rats. We also thank J.A. Chiorini for providing the systems to produce the AAV5-based vectors. This study was partly supported by grants from the Ministry of Education, Culture, Sports, Science and Technology, and the Ministry of Health, Labor and Welfare, Japan; the 'High-Technology Research Center' Project for Private Universities: a matching fund subsidy from the Ministry of Education, Culture, Sports, Science and Technology, 2003-2007; and the 21st Century Centers of Excellence Program from the Ministry of Education, Culture, Sports, Science and Technology.

References

1. Hyman L: Epidemiology of eye disease in the elderly. Eye 1: 330-341, 1987.
2. Klein BE and Klein R: Ocular problems in older Americans with diabetes. Clin Geriatr Med 6: 827-837, 1990.
3. King H and Rewers M: Global estimates for prevalence of diabetes mellitus and impaired glucose tolerance in adults. WHO *Ad Hoc* Diabetes Reporting Group. Diabetes Care 16: 157-177, 1993.
4. Hotta N, Nakamura J, Sakakibara F, *et al*: Electroretinogram in sucrose-fed diabetic rats treated with an aldose reductase inhibitor or an anticoagulant. Am J Physiol 273: E965-E971, 1997.
5. Robison WG Jr, Nagata M, Tillis TN, Laver N and Kinoshita JH: Aldose reductase and pericyte-endothelial cell contacts in retina and optic nerve. Invest Ophthalmol Vis Sci 30: 2293-2299, 1989.

6. Aiello LP, Bursell SE, Clermont A, *et al*: Vascular endothelial growth factor-induced retinal permeability is mediated by protein kinase C *in vivo* and suppressed by an orally effective beta-isoform-selective inhibitor. Diabetes 46: 1473-1480, 1997.
7. Lee TS, MacGregor LC, Fluharty SJ and King GL: Differential regulation of protein kinase C and (Na,K)-adenosine triphosphatase activities by elevated glucose levels in retinal capillary endothelial cells. J Clin Invest 83: 90-94, 1989.
8. Nakamura J, Kato K, Hamada Y, *et al*: A protein kinase C-beta-selective inhibitor ameliorates neural dysfunction in streptozotocin-induced diabetic rats. Diabetes 48: 2090-2095, 1999.
9. Hammes HP, Wellensiek B, Kloting I, Sickel E, Bretzel RG and Brownlee M: The relationship of glycaemic level to advanced glycation end-product (AGE) accumulation and retinal pathology in the spontaneous diabetic hamster. Diabetologia 41: 165-170, 1998.
10. Murata T, Nagai R, Ishibashi T, Inomuta H, Ikeda K and Horiuchi S: The relationship between accumulation of advanced glycation end products and expression of vascular endothelial growth factor in human diabetic retinas. Diabetologia 40: 764-769, 1997.
11. Aiello LP: Vascular endothelial growth factor and the eye: biochemical mechanisms of action and implications for novel therapies. Ophthalmic Res 29: 354-362, 1997.
12. Aiello LP, Avery RL, Arrigg PG, *et al*: Vascular endothelial growth factor in ocular fluid of patients with diabetic retinopathy and other retinal disorders. N Engl J Med 331: 1480-1487, 1994.
13. Ozaki H, Seo MS, Ozaki K, *et al*: Blockade of vascular endothelial cell growth factor receptor signaling is sufficient to completely prevent retinal neovascularization. Am J Pathol 156: 697-707, 2000.
14. Ferrara N, Houck K, Jakeman L and Leung DW: Molecular and biological properties of the vascular endothelial growth factor family of proteins. Endocr Rev 13: 18-32, 1992.
15. Jakeman LB, Winer J, Bennett GL, Altar CA and Ferrara N: Binding sites for vascular endothelial growth factor are localized on endothelial cells in adult rat tissues. J Clin Invest 89: 244-253, 1992.
16. Senger DR, Perruzzi CA, Feder J and Dvorak HF: A highly conserved vascular permeability factor secreted by a variety of human and rodent tumor cell lines. Cancer Res 46: 5629-5632, 1986.
17. Thieme H, Aiello LP, Takagi H, Ferrara N and King GL: Comparative analysis of vascular endothelial growth factor receptors on retinal and aortic vascular endothelial cells. Diabetes 44: 98-103, 1995.
18. Adamis AP, Miller JW, Bernal MT, *et al*: Increased vascular endothelial growth factor levels in the vitreous of eyes with proliferative diabetic retinopathy. Am J Ophthalmol 118: 445-450, 1994.
19. Boulton M, Gregor Z, McLeod D, *et al*: Intravitreal growth factors in proliferative diabetic retinopathy: correlation with neovascular activity and glycaemic management. Br J Ophthalmol 81: 228-233, 1997.
20. Okamoto N, Tobe T, Hackett SF, *et al*: Transgenic mice with increased expression of vascular endothelial growth factor in the retina: a new model of intraretinal and subretinal neovascularization. Am J Pathol 151: 281-291, 1997.
21. Adamis AP, Shima DT, Tolentino MJ, *et al*: Inhibition of vascular endothelial growth factor prevents retinal ischemia-associated iris neovascularization in a nonhuman primate. Arch Ophthalmol 114: 66-71, 1996.
22. Robinson GS, Pierce EA, Rook SL, Foley E, Webb R and Smith LE: Oligodeoxynucleotides inhibit retinal neovascularization in a murine model of proliferative retinopathy. Proc Natl Acad Sci USA 93: 4851-4856, 1996.
23. Aiello LP, Pierce EA, Foley ED, *et al*: Suppression of retinal neovascularization *in vivo* by inhibition of vascular endothelial growth factor (VEGF) using soluble VEGF-receptor chimeric proteins. Proc Natl Acad Sci USA 92: 10457-10461, 1995.
24. Goldman CK, Kendall RL, Cabrera G, *et al*: Paracrine expression of a native soluble vascular endothelial growth factor receptor inhibits tumor growth, metastasis, and mortality rate. Proc Natl Acad Sci USA 95: 8795-8800, 1998.
25. Hasumi Y, Mizukami H, Urabe M, *et al*: Soluble FLT-1 expression suppresses carcinomatous ascites in nude mice bearing ovarian cancer. Cancer Res 62: 2019-2023, 2002.
26. Kendall RL and Thomas KA: Inhibition of vascular endothelial cell growth factor activity by an endogenously encoded soluble receptor. Proc Natl Acad Sci USA 90: 10705-10709, 1993.
27. Kong HL, Hecht D, Song W, *et al*: Regional suppression of tumor growth by *in vivo* transfer of a cDNA encoding a secreted form of the extracellular domain of the flt-1 vascular endothelial growth factor receptor. Hum Gene Ther 9: 823-833, 1998.
28. Shiose S, Sakamoto T, Yoshikawa H, *et al*: Gene transfer of a soluble receptor of VEGF inhibits the growth of experimental eyelid malignant melanoma. Invest Ophthalmol Vis Sci 41: 2395-2403, 2000.
29. Kendall RL, Wang G and Thomas KA: Identification of a natural soluble form of the vascular endothelial growth factor receptor, FLT-1, and its heterodimerization with KDR. Biochem Biophys Res Commun 226: 324-328, 1996.
30. Bainbridge JW, Mistry A, De Alwis M, *et al*: Inhibition of retinal neovascularisation by gene transfer of soluble VEGF receptor sFlt-1. Gene Ther 9: 320-326, 2002.
31. Honda M, Sakamoto T, Ishibashi T, Inomata H and Ueno H: Experimental subretinal neovascularization is inhibited by adenovirus-mediated soluble VEGF/flt-1 receptor gene transfection: a role of VEGF and possible treatment for SRN in age-related macular degeneration. Gene Ther 7: 978-985, 2000.
32. Shinohara M, Masuyama T, Shoda T, *et al*: A new spontaneously diabetic non-obese Torii rat strain with severe ocular complications. Int J Exp Diabetes Res 1: 89-100, 2000.
33. Kakehashi A, Saito Y, Mori K, *et al*: Characteristics of diabetic retinopathy in SDT rats. Diabetes Metab Res Rev (Epub ahead of print March 30, 2006).
34. Dudus L, Anand V, Acland GM, *et al*: Persistent transgene product in retina, optic nerve and brain after intraocular injection of rAAV. Vision Res 39: 2545-2553, 1999.
35. Martin KR, Klein RL and Quigley HA: Gene delivery to the eye using adeno-associated viral vectors. Methods 28: 267-275, 2002.
36. Auricchio A, Behling KC, Maguire AM, *et al*: Inhibition of retinal neovascularization by intraocular viral-mediated delivery of anti-angiogenic agents. Mol Ther 6: 490-494, 2002.
37. Lotery AJ, Yang GS, Mullins RF, *et al*: Adeno-associated virus type 5: transduction efficiency and cell-type specificity in the primate retina. Hum Gene Ther 14: 1663-1671, 2003.
38. Rabinowitz JE, Rolling F, Li C, *et al*: Cross-packaging of a single adeno-associated virus (AAV) type 2 vector genome into multiple AAV serotypes enables transduction with broad specificity. J Virol 76: 791-801, 2002.
39. Yang GS, Schmidt M, Yan Z, *et al*: Virus-mediated transduction of murine retina with adeno-associated virus: effects of viral capsid and genome size. J Virol 76: 7651-7660, 2002.
40. Yoshimura I, Mizuguchi Y, Miyajima A, Asano T, Tadakuma T and Hayakawa M: Suppression of lung metastasis of renal cell carcinoma by the intramuscular gene transfer of a soluble form of vascular endothelial growth factor receptor I. J Urol 171: 2467-2470, 2004.
41. Zhang M, Volpert O, Shi YH and Bouck N: Maspin is an angiogenesis inhibitor. Nat Med 6: 196-199, 2000.
42. Hermens WT, ter Brake O, Dijkhuizen PA, *et al*: Purification of recombinant adeno-associated virus by iodixanol gradient ultracentrifugation allows rapid and reproducible preparation of vector stocks for gene transfer in the nervous system. Hum Gene Ther 10: 1885-1891, 1999.
43. Zolotukhin S, Byrne BJ, Mason E, *et al*: Recombinant adeno-associated virus purification using novel methods improves infectious titer and yield. Gene Ther 6: 973-985, 1999.
44. Kadof PF, Takahashi Y, Wyman M, Ferris F III: Diabetes-like proliferative retinal changes in galactose-fed dogs. Arch Ophthalmol 113: 352-354, 1995.
45. Casey R and Li WW: Factors controlling ocular angiogenesis. Am J Ophthalmol 124: 521-529, 1997.

Circulation Research
JOURNAL OF THE AMERICAN HEART ASSOCIATION

American Heart Association.
Learn and Live.

Interleukin-10 Expression Mediated by an Adeno-Associated Virus Vector Prevents Monocrotaline-Induced Pulmonary Arterial Hypertension in Rats

Takayuki Ito, Takashi Okada, Hiroshi Miyashita, Tatsuya Nomoto, Mutsuko Nonaka-Sarukawa, Ryosuke Uchibori, Yoshikazu Maeda, Masashi Urabe, Hiroaki Mizukami, Akihiro Kume, Masafumi Takahashi, Uichi Ikeda, Kazuyuki Shimada and Keiya Ozawa

Circ. Res. 2007;101;734-741; originally published online Aug 2, 2007;
DOI: 10.1161/CIRCRESAHA.107.153023
Circulation Research is published by the American Heart Association. 7272 Greenville Avenue, Dallas, TX 72514
 Print ISSN: 0009-7330. Online ISSN: 1524-4571

Interleukin-10 Expression Mediated by an Adeno-Associated Virus Vector Prevents Monocrotaline-Induced Pulmonary Arterial Hypertension in Rats

Takayuki Ito, Takashi Okada, Hiroshi Miyashita, Tatsuya Nomoto, Mutsuko Nonaka-Sarukawa, Ryosuke Uchibori, Yoshikazu Maeda, Masashi Urabe, Hiroaki Mizukami, Akihiro Kume, Masafumi Takahashi, Uichi Ikeda, Kazuyuki Shimada, Keiya Ozawa

Abstract—Pulmonary arterial hypertension (PAH) is a fatal disease associated with inflammation and pathological remodeling of the pulmonary artery (PA). Interleukin (IL)-10 is a pleiotropic antiinflammatory cytokine with vasculoprotective properties. Here, we report the preventive effects of IL-10 on monocrotaline-induced PAH. Three-week-old Wistar rats were intramuscularly injected with an adeno-associated virus serotype 1 vector expressing IL-10, followed by monocrotaline injection at 7 weeks old. IL-10 transduction significantly improved survival rates of the PAH rats 8 weeks after monocrotaline administration compared with control gene transduction (75% versus 0%, $P<0.01$). IL-10 also significantly reduced mean PA pressure (22.8 ± 1.5 versus 29.7 ± 2.8 mm Hg, $P<0.05$), a weight ratio of right ventricle to left ventricle plus septum (0.35 ± 0.04 versus 0.42 ± 0.05, $P<0.05$), and percent medial thickness of the PA ($12.9\pm0.3\%$ versus $21.4\pm0.4\%$, $P<0.01$) compared with controls. IL-10 significantly reduced macrophage infiltration and vascular cell proliferation in the remodeled PA in vivo. It also significantly decreased the lung levels of transforming growth factor-β_1 and IL-6, which are indicative of PA remodeling. In addition, IL-10 increased the lung level of heme oxygenase-1, which strongly prevents PA remodeling. In vitro analysis revealed that IL-10 significantly inhibited excessive proliferation of cultured human PA smooth muscle cells treated with transforming growth factor-β_1 or the heme oxygenase inhibitor tin protoporphyrin IX. Thus, IL-10 prevented the development of monocrotaline-induced PAH, and these results provide new insights into the molecular mechanisms of human PAH. (***Circ Res.*** **2007;101:734-741.)**

Key Words: pulmonary hypertension ■ interleukins ■ gene therapy ■ inflammation ■ vascular smooth muscle cell proliferation

Pulmonary arterial hypertension (PAH) is an intractable disease that leads to increased pulmonary arterial pressure, progressive right heart failure, and premature death; however, no satisfactory treatment for PAH has been established.[1] The pathological process of PAH is characterized by abnormal remodeling of the pulmonary artery (PA) associated with excessive proliferation of pulmonary arterial smooth muscle cells (PASMCs).[2] Accumulating evidence suggests important roles of vascular inflammation in its pathogenesis.[2,3] For instance, serum levels of proinflammatory cytokines such as interleukin (IL)-1 and IL-6 reflect the disease activity in patients with idiopathic PAH.[4] Furthermore, injection of IL-6 can produce PAH and PA remodeling in rats.[5] The remodeled PA presents macrophage infiltration and increased expression of a variety of cytokines, including IL-6, tumor necrosis factor (TNF)-α, and transforming growth factor (TGF)-β_1.[6,7] Administration of steroids or immunosuppressive drugs decreases the level of PA pressure in patients with PAH.[8,9] These observations suggest a therapeutic potential of targeting inflammation to prevent PAH progression.[10] However, the precise mechanisms underlying the antiinflammatory effects on PA remodeling have not yet been fully investigated.

IL-10 is a multifunctional antiinflammatory cytokine with a vasculoprotective property. During the course of inflammation, IL-10 is produced by type-2 helper T (Th2) lymphocytes, and it inhibits the production of various proinflammatory cytokines in macrophages and Th1 lymphocytes.[11] Exogenous IL-10 prevents proliferative vasculopathy in vivo by inhibiting inflammatory cell infiltration,[12] smooth muscle cell proliferation,[12,13] and chemokine expression.[14] However, clinical efficacy of systemic recombinant IL-10 administra-

Original received March 28, 2007; revision received July 12, 2007; accepted July 23, 2007.

From the Division of Genetic Therapeutics (T.I., T.N., M.N.-S., M.U., H.M., A.K., K.O., R.U.), the Division of Cardiovascular Medicine (T.I., H.M., M.N.-S., K.S., Y.M.), Jichi Medical University, Japan; the Department of Molecular Therapy (T.O.), National Institute of Neuroscience, National Center of Neurology and Psychiatry, Japan; and the Department of Organ Regeneration (M.T., U.I.), Shinshu University Graduate School of Medicine, Japan.

Correspondence to Takayuki Ito, MD, PhD, Division of Genetic Therapeutics, Jichi Medical University, 3311-1 Yakushiji, Shimotsuke, Tochigi 329-0498, Japan. E-mail titou@jichi.ac.jp

Circulation Research is available at http://circres.ahajournals.org

DOI: 10.1161/CIRCRESAHA.107.153023

tion are insufficient because of the lower local IL-10 levels resulting from its short bioactive half-life.[15] In this study, we used an adeno-associated virus (AAV) vector for IL-10 expression because it is an efficient vehicle for systemic and sustained expression of therapeutic proteins.[14] It also has an advantage over other viral vectors in the therapeutic or mechanistic analysis because it produces minimal inflammatory and immune responses in vivo.

Recently, heme oxygenase (HO)-1, an inducible form of HO that promotes production of a vasodilator carbon monoxide (CO), was shown to mediate antiinflammatory and antiproliferative effects of IL-10 in a model of chronic vasculopathy.[12] Increased HO-1 and CO levels attenuated PAH and PA remodeling by inhibiting PASMC proliferation.[16–18] However, no study has explored a direct link between IL-10 and HO-1 in the pathogenesis of PAH. Thus, we examined the effects of IL-10, delivered via an AAV vector, on PA remodeling in a widely-used rat model of PAH induced by the pyrolizidine alkaloid monocrotaline (MCT). We also investigated the mechanisms underlying the effects of IL-10 on the following factors involved in the inflammatory and proliferative vascular changes in PAH: PASMC, macrophage, TGF-β_1, IL-6, and HO-1.

Materials and Methods

AAV Vector Production

DNA encoding rat IL-10 was polymerase chain reaction-amplified from rat splenocyte complementary DNA, using the primers 5′-GCACGAGAGCCACAACGCA-3′ and 5′-GATTTGAGTACG-ATCCATTTATTCAAAACGAGGAT-3′. For efficient transgene expression in the skeletal muscle, we constructed a recombinant AAV vector which carried the IL-10 gene (AAV-IL-10) or enhanced green fluorescent protein (eGFP) gene (AAV-eGFP), controlled by the modified chicken β-actin promoter with the cytomegalo virus-immediate early enhancer and the woodchuck hepatitis virus post-transcriptional regulatory element (a kind gift from Dr Thomas Hope, Infectious Disease Laboratory, Salk Institute). AAV vectors were prepared according to the previously described 3-plasmid transfection adenovirus-free protocol with minor modifications to use the active gassing system.[19,20] In brief, 60% confluent human embryonic kidney 293 cells incubated in a large culture vessel with active air circulation were cotransfected with the proviral transgene plasmid, AAV-1 chimeric helper plasmid (p1RepCap), and adenoviral helper plasmid pAdeno (Avigen Inc). The crude viral lysate was purified by 2 rounds of cesium chloride 2-tier centrifugation.[21] The viral stock titer was determined against plasmid standards by dot blot hybridization, after which the stock was dissolved in HN buffer (50 mmol/L HEPES, pH 7.4, 0.15 mol/L NaCl) before injection.

Animal Models

All animal experiments were approved by the Jichi Medical University ethics committee and were performed in accordance with the *National Institute of Health Guide for the Care and Use of Laboratory Animals*. To evaluate the efficiency of in vivo gene expression, 3-week-old male Wistar rats (Clea Japan Inc, Tokyo, Japan) weighing 45 to 55 g were injected with AAV-IL-10 (200 μL, 3×10^{10} to 1×10^{11} genome copies [g.c.] per body) into the bilateral anterior tibial muscles (n=3 animals per group). For hemodynamic and histological analysis, we randomly formed 4 groups comprising 5 rats each: sham rats that were administered the HN buffer (1, NC group); MCT-treated rats administered the HN buffer (2, MCT group); MCT rats administered AAV-eGFP (3, MCT+eGFP group); and MCT rats administered AAV-IL-10 (4, MCT+IL-10 group). After anesthetized with a spontaneous inhalation of 1% isoflurane, the rats in the groups 3 and 4 received intramuscular injection of AAV-eGFP or AAV-IL-10 (200 μL, 6×10^{10} g.c. per body), respectively. Rats in groups 1 and 2 were injected with the HN buffer (200 μL). MCT (Wako Pure Chemicals) was dissolved in 0.1N HCl, and the pH adjusted to 7.4 with 1.0N NaOH. For hemodynamic and histological studies, all rats except those in the NC group were subcutaneously injected with MCT (30 mg/kg) under the spontaneous inhalation of 1% isoflurane at 4 weeks after vector treatment. For the survival study, rats (n=8 animals/group) were injected with a lethal dose of MCT (45 mg/kg) under the spontaneous inhalation of 1% isoflurane at 4 weeks after vector injection. Survival was estimated from the date of MCT injection until death or 8 weeks after injection.

Hemodynamic Analysis

Four weeks after MCT injection, the rats were anesthetized with spontaneous inhalation of 1% isoflurane, and a tracheotomy was performed. Then, they were mechanically ventilated using a respirator (SAR-830/AP, CWE; tidal volume: 10 mL/kg, respiratory rate: 30 breaths per min) and anesthetized with 0.5% isoflurane through a tracheostomy. After the thoracic cavity was opened using a midsternal approach, 2.0F high-fidelity manometer-tipped catheters (SPC-320, Millar Instruments Inc) were inserted directly into the right or left ventricle. The mean pulmonary arterial pressure (mPAP) or mean aortic arterial pressure (mAoP) was measured using the catheters that were advanced from the right or left ventricle, respectively. The heart rate (HR) was measured by unipolar lead electrocardiography.

Ventricular Weight Measurement and Morphometric Analysis of the PA

After hemodynamic analysis, the rats were euthanized using an overdose isoflurane (5%). The lungs and PAs were perfused with 5 mL of saline followed by 10 mL of cold 4% paraformaldehyde. Each ventricle and the lungs were excised, dissected free, and weighed. The weight ratio of right ventricle to the left ventricle plus septum [RV/(LV+S)] was calculated as an index of right ventricular hypertrophy (RVH). The tissues were fixed in 4% paraformaldehyde for 4 hours, transferred to 30% sucrose in 0.1 mol/L phosphate buffer (pH 7.4) for cryoprotection, and stored at 4°C overnight. Lung tissue was frozen in Tissue-Tek OCT compound (Sakura Finetechnical Co) at −20°C. Then, 7-μm sections were cut using a cryostat. Hematoxylin and eosin (HE) staining was performed on sections from the middle lobe of the right lung, and these were examined using light microscopy. Morphometric analysis was performed in PAs with an external diameter of 25 to 50 and 51 to 100 μm. The medial wall thickness was calculated with the following formula: medial thickness (%)=medial wall thickness/external diameter×100.[22] For quantitative analysis, 30 vessels from each rat were counted and the average was calculated.

Immunohistochemistry

Immunohistochemical staining was performed with monoclonal antibodies against ED1 (1:100; Serotec) and proliferating cell nuclear antigen (PCNA, 1:200; Zymed), using the streptavidin-biotin-peroxidase method, as described previously.[23] ED1 recognizes the lysosomal membrane antigen expressed by a majority of tissue macrophages. Irrelevant mouse immunoglobulin G (Vector Laboratories) was used as a negative control. Reactions were visualized using Vector SG (Vector Laboratories) or 3,3′-diaminobenzidine (Zymed) and counterstained with nuclear fast red or hematoxylin. The number of ED1-positive cells was counted in 250×250-μm fields under 400× magnification and expressed as cells per mm^2. The number of PCNA-positive cells was quantitatively evaluated as a percentage of total vascular cells in the fields under 1000× magnification. For each rat, the average number or percentage of each cell in 15 randomly selected fields was used for statistical analysis.

Protein Assay

Protein samples were prepared by homogenization of the frozen lung tissue in lysis buffer [10 μmol/L Tris/Cl (pH 8.0), 0.2% NP-40,

1 μmol/L EDTA (pH 7.6)] supplemented with protease inhibitor cocktail Complete Mini (Roche Diagnostics). After centrifugation of the homogenates (3000*g* for 10 minutes), the supernatants or serum samples were used for measurement. To activate latent TGF-β_1 to an immunoreactive form, the samples were treated with acid according to the manufacturer's instructions (R&D Systems Inc). IL-10 or IL-6 concentrations in the sera and TGF-β_1, IL-6, HO-1, or TNF-α in the lung extracts were measured using enzyme-linked immunosorbent assay (ELISA) kits (Amersham Pharmacia Biotech; R&D Systems). The minimum detectable dose was 3, 3, 16, and 5 pg/mL or 0.78 ng/mL for IL-10, TGF-β_1, IL-6, and TNF-α, or HO-1, respectively. Inter- and intraassay precision of these kits was <10%. The total protein concentrations in the lung extracts were estimated using a BCA Protein Assay kit (PIERCE). The levels of TGF-β_1, IL-6, HO-1, or TNF-α in the lung were expressed as pg per mg protein.

Cell Culture and Proliferation Assay

Human PASMCs were obtained from Clonetics Corp and grown in SmGM-2 medium (Clonetics Corp). PASMCs with a passage between 4 and 6 were used in the experiments. Cells (1×10^3 per well) were incubated in 96-well plates with serum-free Dulbecco's modified Eagle's medium and nutrient mixture F12 (DMEM-F12, Invitrogen) in an atmosphere of 5% CO_2 in the air at 37°C. A tetrazolium-based colorimetric proliferation assay (XTT assay; Cell Proliferation Kit II, Roche Diagnostics) was performed 2 days after adding tin protoporphyrin IX (SnPP; Frontier Scientific), human recombinant TGF-β_1, IL-6, or IL-10 (PeproTech Inc). The optical density between 450 and 650 nm were measured to estimate the number of viable cells.

Statistical Analysis

Data from multiple experiments are expressed as mean±SEM. Statistical analysis and correlations were performed using StatView (Abacus Concepts, Inc). Survival curves were analyzed using the Kaplan–Meier method and compared by log-rank tests. Differences in other parameters were evaluated by analysis of variance combined with Fisher test. The correlation test was used to measure the association between 2 variables. A value of $P<0.05$ was considered statistically significant.

Results

AAV Vector-Mediated IL-10 Expression Improves Survival of MCT-PAH Rats

Eight weeks after AAV-IL-10 injection, serum IL-10 concentrations were elevated in a vector dose-dependent manner (Figure 1A). We determined that injection with AAV-IL-10 (6×10^{10} g.c. per rat) significantly increased serum IL-10 levels as compared with untreated controls (184.1±47.6 versus 18.8±1.3 pg/mL, $P<0.05$, n=3 each). In contrast, injection with MCT (Figure 1A) or AAV-eGFP alone (data not shown) caused no significant change in serum IL-10 levels. Therefore, we used this dosage for all vectors in subsequent experiments. For survival analysis, the rats were injected with a lethal dose of MCT, after 4 weeks of vector injection. The survival in IL-10–transduced rats was significantly improved as compared with the eGFP-transduced rats 8 weeks after MCT injection (75% versus 0%, $P<0.01$, n=8 each; Figure 1B).

Effects of IL-10 on PAH and RVH

Four weeks after MCT injection, the mPAP levels were significantly higher than those of the untreated controls (30.1±4.0 versus 20.0±2.1 mm Hg, $P<0.01$, n=5 each; Figure 2A). Treatment with AAV-IL-10 but not AAV-eGFP significantly inhibited the elevation of mPAP (22.8±1.5

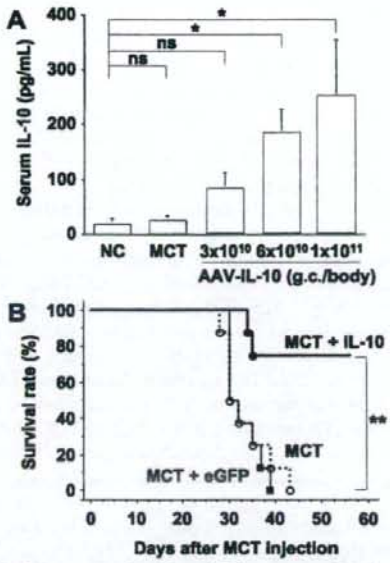

Figure 1. Adeno-associated virus (AAV) vector-mediated systemic interleukin (IL)-10 expression improves survival of monocrotaline (MCT)-induced pulmonary arterial hypertension (PAH) rats. A, In vivo IL-10 expression induced by AAV-IL-10. Serum IL-10 concentrations (pg/mL) were determined using ELISA 8 weeks after a single intramuscular injection of AAV-IL-10 into the anterior tibial muscles of 3-week-old Wistar rats. Genome copies (g.c.) per rat were as indicated. Data represent mean±SEM (n=3 animals per group, *$P<0.05$). ns indicates not statistically significant; NC, untreated controls. B, The Kaplan-Meier survival curve in MCT-PAH rats. The Wistar rats were treated with a lethal dose of MCT 4 weeks after the single intramuscular injection of HN buffer (MCT group), AAV-eGFP (MCT+eGFP group), or AAV-IL-10 (MCT+IL-10 group). n=8 animals per group, **$P<0.01$ versus MCT or MCT+eGFP groups.

versus 29.7±2.8 mm Hg, $P<0.01$, n=5 each; Figure 2A). Moreover, serum IL-10 concentrations correlated negatively with mPAP in MCT-treated rats ($r=-0.75$, $P<0.01$, n=15; Figure 2B). In contrast, this IL-10 expression caused no significant change in HR (data not shown) and mAoP (76.7±2.1 versus 74.6±6.8 mm Hg, MCT+IL-10 versus MCT+eGFP group, n=5 each). IL-10 expression also has a beneficial effect on RVH. Four-week MCT treatment significantly increased the RV/(LV+S) values as compared with the untreated controls ($P<0.01$, n=5 each; Figure 2C). Treatment with AAV-IL-10 but not AAV-eGFP inhibited MCT-induced increase of RV/(LV+S) significantly ($P<0.05$, n=5 each; Figure 2C). Furthermore, serum IL-10 concentrations correlated negatively with RV/(LV+S) in MCT-treated rats ($r=-0.57$, $P<0.05$, n=15; Figure 2D). These results indicate that sustained IL-10 expression prevented the development of MCT-induced PAH and RVH.

Effects of IL-10 on Histological Changes of the PA

Medial hypertrophy is a hallmark of pathological vascular remodeling in PAH. Four weeks after MCT injection, the medial thickness of PAs was markedly increased in the MCT-treated rats compared with untreated controls ($P<0.01$,

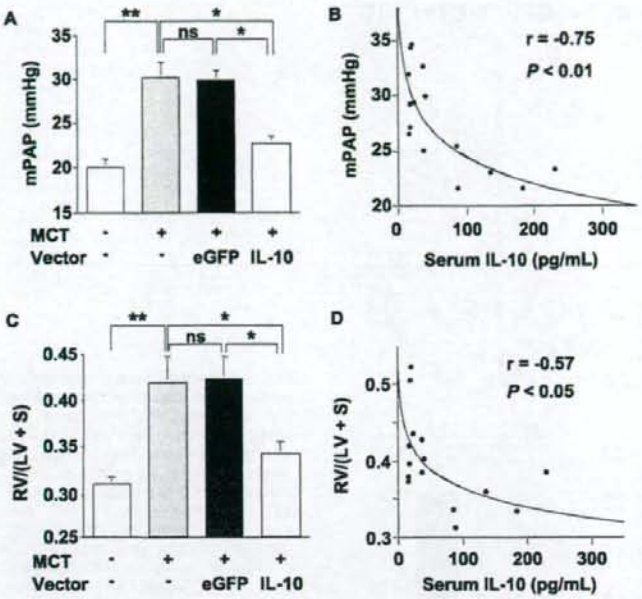

Figure 2. Effects of IL-10 on PAH and right ventricular hypertrophy (RVH). The 7-week-old Wistar rats were treated with monocrotaline (MCT) 4 weeks after vector injection. A, Statistical analysis of mean pulmonary arterial pressure (mPAP, mm Hg) determined by direct catheterization 4 weeks after MCT injection. Data represent the mean±SEM (n=5 animals per group; *$P<0.05$, **$P<0.01$). ns indicates not statistically significant. B, Correlation between serum IL-10 concentrations and mPAP levels in the MCT-treated rats (groups: MCT, MCT+eGFP, or MCT+IL-10; n=5 animals per group; $r=-0.75$, $P<0.01$). C, Quantitative RVH analysis. The weight ratio of the right ventricle to left ventricle plus septum [RV/(LV+S)] is presented as an index of RVH (n=5 animals per group; *$P<0.05$, **$P<0.01$). D, Correlation between serum IL-10 concentrations and RV/(LV+S) in the MCT-treated rats (groups: MCT, MCT+eGFP, and MCT+IL-10; n=5 animals per group; $r=-0.57$, $P<0.05$).

n=5 each; Figure 3B, 25 to 50 μm; Figure 3C, 51 to 100 μm in external diameter). Treatment with AAV-IL-10 but not AAV-eGFP significantly inhibited the increase in percent medial thickness ($P<0.01$, n=5 each). Inflammatory cell infiltration and vascular cell proliferation are also important indicators in the progression of PA remodeling. Immunohistochemical analysis shows that treatment with AAV-IL-10 significantly decreased the number of accumulated macrophages (ED1-positive cells; $P<0.01$, n=5 each; Figure 3D) and proliferating vascular cells (PCNA-positive cells; $P<0.01$, n=5 each; Figure 3E) in the PA of MCT-treated rats as compared with treatment with MCT alone or AAV-eGFP.

Effects of IL-10 on Cytokine Expression

We analyzed pulmonary tissue and serum cytokine levels relevant to the pathogenesis of PAH. Four weeks after MCT injection, the TGF-β_1 and IL-6 levels in the MCT-treated rats were significantly higher than those of the untreated controls ($P<0.01$, n=5 each; Figure 4A and 4C). Treatment with AAV-IL-10 but not AAV-eGFP significantly inhibited the MCT-induced elevation of TGF-β1 and IL-6 levels ($P<0.01$, n=5 each). Furthermore, these levels correlated positively with the percent medial thickness in the rats with or without MCT treatment ($r=0.84$, $P<0.01$; $r=0.87$, $P<0.01$, respectively; Figure 4B and 4D).

HO-1 has been reported to mediate the antiinflammatory effects of IL-10.[24] Treatment with AAV-IL-10 but not AAV-eGFP or MCT alone significantly increased the lung HO-1 levels as compared with untreated controls ($P<0.05$, n=5 each, Figure 4E). In addition, HO-1 levels correlated negatively with IL-6 levels in MCT-treated rats ($r=-0.85$, $P<0.01$; Figure 4F). In contrast, serum IL-6 levels positively correlated with lung IL-6 levels ($r=-0.69$, $P<0.01$; Figure 4G). Although the lung TNF-α levels significantly increased in MCT-treated rats compared with untreated controls, IL-10 expression caused no change in the lung TNF-α levels (Figure 4H).

Effects of IL-10 on PASMC Proliferation

To determine whether IL-10 directly inhibits PASMC proliferation, we performed an in vitro colorimetric XTT assay using cultured human PASMCs. Treatment of PASMCs with SnPP, which inactivates HO-1, and treatment with TGF-β_1 or IL-6 dose dependently promoted cell proliferation (n=4 each, $P<0.05$; Figure 5A through 5C). Treatment with IL-10 alone had no significant effect on PASMC proliferation (Figure 5D). On the other hand, pretreatment with IL-10 significantly inhibited PASMC proliferation induced by SnPP or TGF-β_1 (n=4 each, $P<0.05$; Figure 5E) but not that induced by IL-6.

Discussion

The present study demonstrates that IL-10, delivered by an intramuscular injection of an AAV1 vector, prevented the development of MCT-PAH in rats. Systemic IL-10 expression also improved survival in rats and prevented the development of RVH and medial hypertrophy of PA. IL-10 also reduced macrophage accumulation, vascular cell proliferation, and pulmonary tissue levels of TGF-β_1 and IL-6, all of which play pivotal roles in progression of PA remodeling. Further, IL-10 enhanced HO-1 levels in the lung. Thus, IL-10 exerts multiple preventive effects on inflammatory and proliferative PA remodeling (Figure 6).

Blockade of a single proinflammatory signaling pathway by IL-1 or monocyte chemoattractant protein-1 attenuates PA remodeling.[25,26] However, the prosurvival effects of antiinflammatory molecules on PAH animals have not been re-

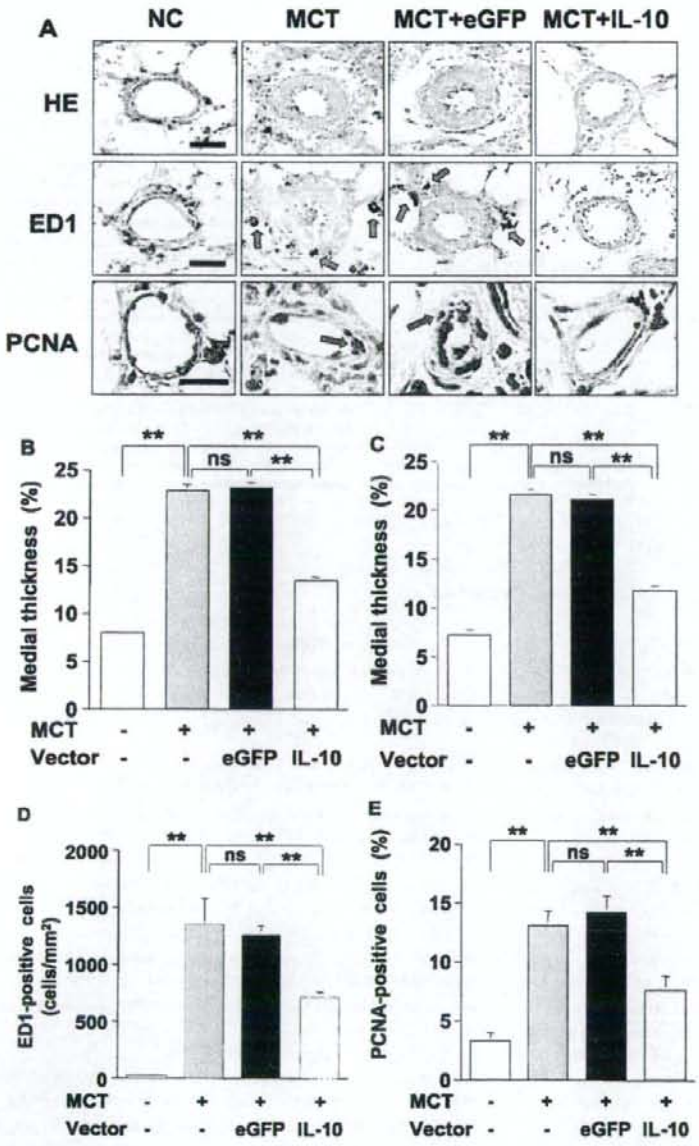

Figure 3. Antiinflammatory and antiproliferative effects of IL-10 on the remodeled pulmonary artery (PA). The 7-week-old Wistar rats were treated with MCT 4 weeks after vector injection. Representative cross-sectional views of the peripheral PAs stained with HE or immunohistochemistry (ED1 or PCNA) 4 weeks after MCT treatment (A; original magnification ×1000, Scale bar=20 μm). Blue arrows indicate ED-1–positive cells and red arrows, PCNA-positive cells. Quantification of percent medial thickness for vessels 25 to 50 μm (B) and 51 to 100 μm (C) in external diameter. Quantitative analysis of the number of perivascular macrophages (ED-1–positive cells, D) and proliferating vascular cells (PCNA-positive cells, E). Data represent mean±SEM (n=5 animals per group, $^{**}P<0.01$). ns indicates not statistically significant.

ported. Evidence of right heart failure is involved in the mortality of MCT-PAH rats. In this study, all rats treated with a lethal dose of MCT exhibited symptoms of right heart failure such as pleural effusion and body weight decrease. In the setting of severe PAH and right heart failure, cytokine networks may orchestrate disease progression. Thus, blockades of multiple inflammatory signals might be responsible for the prosurvival effect of IL-10.

IL-10 has gained significant attention because of its suppressive influence on inflammatory and proliferative vasculopathy. The IL-10 receptor is expressed on vascular smooth muscle cells (VSMCs). IL-10 inhibits inflammation and VSMC proliferation in arterial remodeling after balloon injury or transplant rejection.[12,13] Consistent with previous studies using MCT-PAH,[6,7] we demonstrate that increased levels of TGF-β_1 and IL-6 are related to PASMC proliferation and PA remodeling progression. Although treatment with IL-10 alone caused no significant effects on PASMC proliferation,[27] IL-10 significantly inhibited the lung TGF-β_1 expression and TGF-β_1-induced PASMC proliferation. TGF-β_1 enhances PASMC proliferation of idiopathic PAH patients but not that of normal subjects or secondary PAH patients.[28]

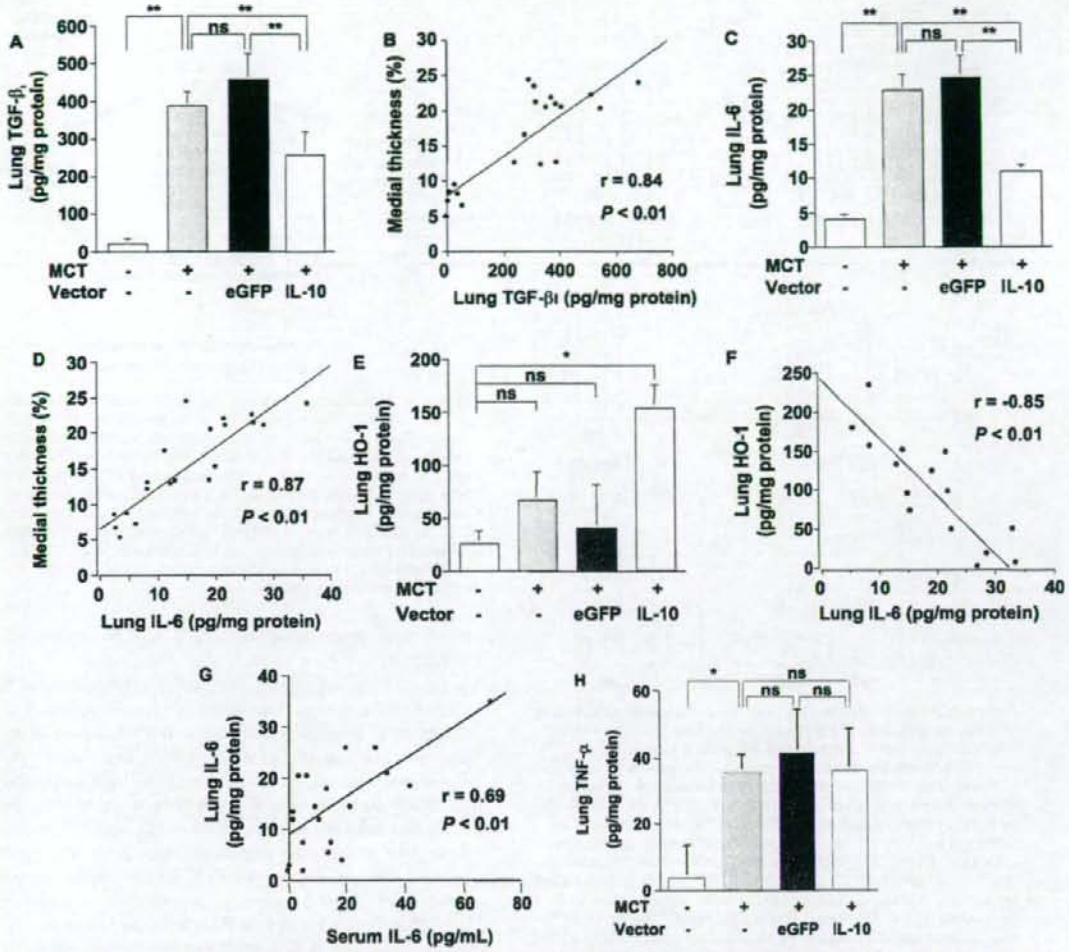

Figure 4. Effects of IL-10 on expression of transforming growth factor-β_1 (TGF-β_1), IL-6, heme oxygenase-1 (HO-1), and tumor necrosis factor-α (TNF-α) in the lung. The 7-week-old Wistar rats were treated with MCT 4 weeks after vector injection. Concentrations of active TGF-β_1 (A), IL-6 (C), HO-1 (E), and TNF-α (H) in the lung extracts were detected using ELISA 4 weeks after MCT treatment. Data represent mean±SEM (n=5 animals per group; *P<0.05, **P<0.01). ns indicates not statistically significant. Correlation between the percent medial thickness and lung levels of TGF-β_1 (B) or IL-6 (D) in rats (groups: NC, MCT, MCT+eGFP, or MCT+IL-10; n=5 animals per group; r=0.84, P<0.01 and r=0.87, P<0.01, respectively). Correlation between the HO-1 and IL-6 (F) levels in the rat lung (groups: MCT, MCT+eGFP, or MCT+IL-10; n=5 animals per group; r=−0.85, P<0.01). Correlation between the lung and serum IL-6 levels (G) in rats (groups: NC, MCT, MCT+eGFP, or MCT+IL-10; n=5 animals per group; r=0.69, P<0.01).

Additionally, TGF-β_1 is accumulated in the hypertrophic PA of both human PAH and MCT-PAH[29,30] and exacerbates PA remodeling.[31]

IL-6, a multifunctional proinflammatory cytokine, acts as a strong mitogen to promote VSMC proliferation.[11] Macrophage infiltration is a hallmark of PAH progression, and activated macrophages produce substantial amounts of IL-6 in MCT-PAH rats.[6,32] In this study, IL-10 treatment inhibited perivascular macrophage infiltration and the lung IL-6 expression in vivo but not IL-6-induced PASMC proliferation in vitro. These results suggest that IL-10 may attenuate IL-6 function indirectly through the decreased accumulation of perivascular macrophages and IL-6. Furthermore, the serum IL-6 levels significantly correlated with the lung IL-6 levels. Because serum IL-6 level reflects the disease activity of idiopathic PAH, it can be a useful biomarker of antiinflammation therapy of PAH. On the other hand, IL-10 did not affect the MCT-induced TNF-α expression in the lung. However, previous studies demonstrated that IL-10 prevents TNF-α–induced VSMC proliferation in vitro.[27] These observations suggest that IL-10 might modulate the downstream signal of TNF-α but not its expression in the setting of MCT-PAH. Overall, IL-10 affects the dynamics of cytokine networks involved in PA remodeling, and its site of action may differ according to the cytokine signal.

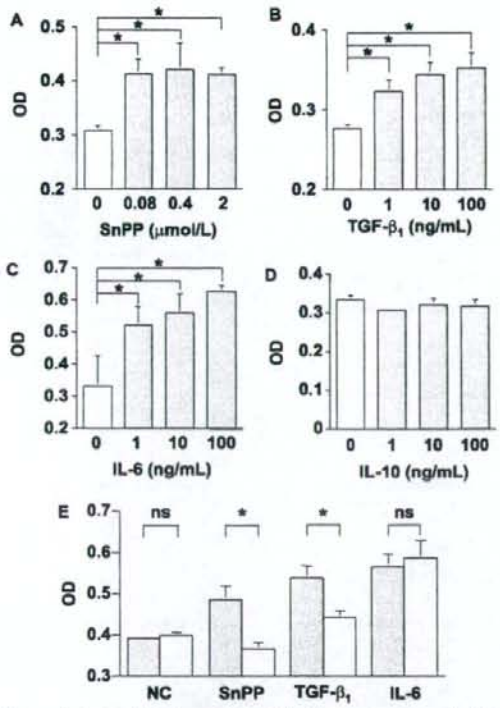

Figure 5. Antiproliferative effects of IL-10 on pulmonary arterial smooth muscle cells (PASMCs). The number of viable human PASMCs cultured in serum-free DMEM-F12 was estimated using a colorimetric assay (XTT assay). The optical density (OD) between 450 nm and 650 nm indicates the extent of cell proliferation. Addition of tin protoporphyrin IX (SnPP, A), TGF-β_1 (B), or IL-6 (C) dose-dependently promotes PASMC proliferation. Although IL-10 alone has no significant effect (D), pretreatment with IL-10 (10 ng/mL) inhibits PASMC proliferation induced by SnPP (2 μmol/L) or TGF-β_1 (20 ng/mL, E) but not that induced by IL-6 (20 ng/mL). Closed columns, cells not treated with IL-10; open columns, IL-10–treated cells. The results are representative of 3 independent experiments. Data represent mean±SEM (n=4 each, *P<0.05). ns indicates not statistically significant.

CO induced by HO-1 blocks PASMC proliferation not only directly by inhibiting the expression of a cell cycle–specific transcription factor but also indirectly by attenuating mitogen signaling.[16] Interestingly, the transgenic mice that constitutively express HO-1 are protected from the development of hypoxia-induced PAH and excessive expression of a mitogen IL-6.[33] In this study, AAV-IL-10 administration increased the HO-1 level that negatively correlated with the IL-6 level in the lung of MCT-PAH rats. These observations suggest a dynamic relationship between IL-6 and HO-1 in PA remodeling progression. Chen et al[12] reported that AAV-IL-10 injection enhanced the activity and protein levels of HO-1, but SnPP treatment that inactivates HO-1 reversed the vasculoprotective effects of IL-10 in vivo. Here, we show that pretreatment with recombinant IL-10 suppressed the excessive PASMC proliferation induced by HO-1 inactivation with SnPP. Thus, IL-10 may sustain CO levels by maintaining

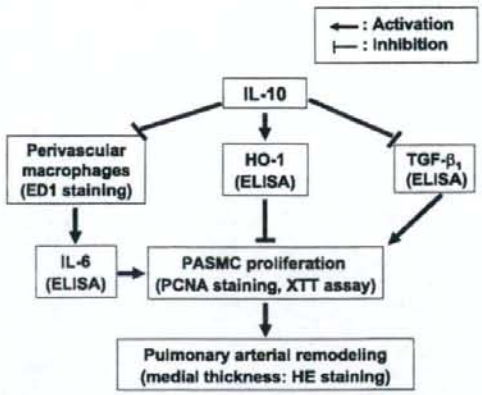

Figure 6. Proposed explanation for IL-10–mediated prevention of PAH and vascular remodeling. Monocrotaline treatment causes PAH in rats by inducing inflammation and proliferation of the PA. IL-10 prevents the development of PAH and PA remodeling by inhibiting vascular inflammation and proliferation. The effects of IL-10 are related to the decreased accumulation of perivascular macrophages and the reduced levels of active TGF-β_1 and IL-6. IL-10 induces HO-1 expression, which can negatively regulate inflammation and proliferation in the PA. IL-10 inhibits abnormal proliferation of PASMCs, thereby preventing PAH development.

HO-1 from inactivating, leading to the prevention of PA remodeling.

Finally, we will discuss the clinical implication and limitations of this study. Consistent with previous studies, maximum gene expression was noted 6 to 8 weeks after the intramuscular injection of AAV vectors. In this study, AAV-IL-10 was injected 4 weeks before MCT administration for the transgene expression to reach plateau levels when MCT-PAH was fully developed (3 to 4 weeks after the injection). Thus, our results are completely based on a prevention protocol, which may be rare in a clinical setting. Intramuscular AAV-IL-10 injection is an attractive candidate for antiinflammation therapy of PAH because inflammatory cytokine expression is associated with the clinical course of the disease. In addition, this strategy exhibited no life-threatening complications such as shock and sepsis which may occur in intravenous prostacyclin infusion therapy. However, therapeutic effects of IL-10 in established PAH has not been determined. Therefore, it should be further examined in studies using a treatment protocol. MCT-PAH is a widely-used and suitable model for exploring inflammatory mechanisms in PAH progression. However, how IL-10 affects other pathogenesis in PAH remains unknown. In the future, IL-10 function needs to be examined in other PAH models such as hypoxia-induced PAH.

In conclusion, AAV vector-mediated sustained IL-10 expression prevented the development of MCT-PAH in rats. The antiremodeling effects of IL-10 are related to the reduction of macrophage infiltration and pathological cytokine expression as well as increased HO-1 levels in the lung. Although the therapeutic role of IL-10 should be further investigated, our results provide new insights into molecular mechanisms underlying the development of human PAH.

Acknowledgments

We thank Miyoko Mitsu for her encouragement and technical support.

Sources of Funding

This work was supported by grants from (1) the Ministry of Health, Labor and Welfare of Japan; (2) Grants-in-Aid for Scientific Research; (3) grant for 21 Century COE Program; (4) "High-Tech Research Center" Project for Private Universities, matching fund subsidy, from the Ministry of Education, Culture, Sports, Science and Technology of Japan; and (5) The Research Award to Jichi Medical School Graduate Student.

Disclosures

None.

References

1. Humbert M, Sitbon O, Simonneau G. Treatment of pulmonary arterial hypertension. *N Engl J Med*. 2004;351:1425–1436.
2. Stenmark KR, Fagan KA, Frid MG. Hypoxia-induced pulmonary vascular remodeling: cellular and molecular mechanisms. *Circ Res*. 2006; 99:675–691.
3. Tuder RM, Groves B, Badesch DB, Voelkel NF. Exuberant endothelial cell growth and elements of inflammation are present in plexiform lesions of pulmonary hypertension. *Am J Pathol*. 1994;144:275–285.
4. Humbert M, Monti G, Brenot F, Sitbon O, Portier A, Grangeot-Keros L, Duroux P, Galanaud P, Simonneau G, Emilie D. Increased interleukin-1 and interleukin-6 serum concentrations in severe primary pulmonary hypertension. *Am J Respir Crit Care Med*. 1995;151:1628–1631.
5. Miyata M, Sakuma F, Yoshimura A, Ishikawa H, Nishimaki T, Kasukawa R. Pulmonary hypertension in rats. 2. Role of interleukin-6. *Int Arch Allergy Immunol*. 1995;108:287–291.
6. Miyata M, Sakuma F, Yoshimura A, Ishikawa H, Nishimaki T, Kasukawa R. Pulmonary hypertension in rats. 1. Role of bromodeoxyuridine-positive mononuclear cells and alveolar macrophages. *Int Arch Allergy Immunol*. 1995;108:281–286.
7. Arcot SS, Lipke DW, Gillespie MN, Olson JW. Alterations of growth factor transcripts in rat lungs during development of monocrotaline-induced pulmonary hypertension. *Biochem Pharmacol*. 1993;46: 1086–1091.
8. Karmochkine M, Wechsler B, Godeau P, Brenot F, Jagot JL, Simonneau G. Improvement of severe pulmonary hypertension in a patient with SLE. *Ann Rheum Dis*. 1996;55:561–562.
9. Bellotto F, Chiavacci P, Laveder F, Angelini A, Thiene G, Marcolongo R. Effective immunosuppressive therapy in a patient with primary pulmonary hypertension. *Thorax*. 1999;54:372–374.
10. Ito T, Ozawa K, Shimada K. Current drug targets and future therapy of pulmonary arterial hypertension. *Curr Med Chem*. 2007;14:719–733.
11. Ito T, Ikeda U. Inflammatory cytokines and cardiovascular disease. *Curr Drug Targets Inflamm Allergy*. 2003;2:257–265.
12. Chen S, Kapturczak MH, Wasserfall C, Glushakova OY, Campbell-Thompson M, Deshane JS, Joseph R, Cruz PE, Hauswirth WW, Madsen KM, Croker BP, Berns KI, Atkinson MA, Flotte TR, Tisher CC, Agarwal A. Interleukin 10 attenuates neointimal proliferation and inflammation in aortic allografts by a heme oxygenase-dependent pathway. *Proc Natl Acad Sci U S A*. 2005;102:7251–7256.
13. Mazighi M, Pelle A, Gonzalez W, Mtairag el M, Philippe M, Henin D, Michel JB, Feldman LJ. IL-10 inhibits vascular smooth muscle cell activation *in vitro* and *in vivo*. *Am J Physiol Heart Circ Physiol*. 2004; 287:H866–H871.
14. Yoshioka T, Okada T, Maeda Y, Ikeda U, Shimpo M, Nomoto T, Takeuchi K, Nonaka-Sarukawa M, Ito T, Takahashi M, Matsushita T, Mizukami H, Hanazono Y, Kume A, Ookawara S, Kawano M, Ishibashi S, Shimada K, Ozawa K. Adeno-associated virus vector-mediated interleukin-10 gene transfer inhibits atherosclerosis in apolipoprotein E-deficient mice. *Gene Ther*. 2004;11:1772–1779.
15. Li MC, He SH. IL-10 and its related cytokines for treatment of inflammatory bowel disease. *World J Gastroenterol*. 2004;10:620–625.
16. Morita T, Mitsialis SA, Koike H, Liu Y, Kourembanas S. Carbon monoxide controls the proliferation of hypoxic vascular smooth muscle cells. *J Biol Chem*. 1997;272:32804–32809.
17. Christou H, Morita T, Hsieh CM, Koike H, Arkonac B, Perrella MA, Kourembanas S. Prevention of hypoxia-induced pulmonary hypertension by enhancement of endogenous heme oxygenase-1 in the rat. *Circ Res*. 2000;86:1224–1229.
18. Yun S, Junbao D, Limin G, Chaomei Z, Xiuying T, Chaoshu T. The regulating effect of heme oxygenase/carbon monoxide on hypoxic pulmonary vascular structural remodeling. *Biochem Biophys Res Commun*. 2003;306:523–529.
19. Matsushita T, Elliger S, Elliger C, Podsakoff G, Villarreal L, Kurtzman GJ, Iwaki Y, Colosi P. Adeno-associated virus vectors can be efficiently produced without helper virus. *Gene Ther*. 1998;5:938–945.
20. Okada T, Nomoto T, Yoshioka T, Nonaka-Sarukawa M, Ito T, Ogura T, Iwata-Okada M, Uchibori R, Shimazaki K, Mizukami H, Kume A, Ozawa K. Large-scale production of recombinant viruses by use of a large culture vessel with active gassing. *Hum Gene Ther*. 2005;16:1212–1218.
21. Okada T, Nomoto T, Shimazaki K, Lijun W, Lu Y, Matsushita T, Mizukami H, Urabe M, Hanazono Y, Kume A, Muramatsu S, Nakano I, Ozawa K. Adeno-associated virus vectors for gene transfer to the brain. *Methods*. 2002;28:237–247.
22. Kay JM, Keane PM, Suyama KL, Gauthier D. Angiotensin converting enzyme activity and evolution of pulmonary vascular disease in rats with monocrotaline pulmonary hypertension. *Thorax*. 1982;37:88–96.
23. Yoshioka T, Ageyama N, Shibata H, Yasu T, Misawa Y, Takeuchi K, Matsui K, Yamamoto K, Terao K, Shimada K, Ikeda U, Ozawa K, Hanazono Y. Repair of infarcted myocardium mediated by transplanted bone marrow-derived CD34$^+$ stem cells in a nonhuman primate model. *Stem Cells*. 2005;23:355–364.
24. Lee TS, Chau LY. Heme oxygenase-1 mediates the anti-inflammatory effect of interleukin-10 in mice. *Nat Med*. 2002;8:240–246.
25. Voelkel NF, Tuder RM, Bridges J, Arend WP. Interleukin-1 receptor antagonist treatment reduces pulmonary hypertension generated in rats by monocrotaline. *Am J Respir Cell Mol Biol*. 1994;11:664–675.
26. Kimura H, Kasahara Y, Kurosu K, Sugito K, Takiguchi Y, Terai M, Mikata A, Natsume M, Mukaida N, Matsushima K, Kuriyama T. Alleviation of monocrotaline-induced pulmonary hypertension by antibodies to monocyte chemotactic and activating factor/monocyte chemoattractant protein-1. *Lab Invest*. 1998;78:571–581.
27. Selzman CH, McIntyre RC Jr, Shames BD, Whitehill TA, Banerjee A, Harken AH. Interleukin-10 inhibits human vascular smooth muscle proliferation. *J Mol Cell Cardiol*. 1998;30:889–896.
28. Morrell NW, Yang X, Upton PD, Jourdan KB, Morgan N, Sheares KK, Trembath RC. Altered growth responses of pulmonary artery smooth muscle cells from patients with primary pulmonary hypertension to transforming growth factor-β_1 and bone morphogenetic proteins. *Circulation*. 2001;104:790–795.
29. Botney MD, Bahadori L, Gold LI. Vascular remodeling in primary pulmonary hypertension. Potential role for transforming growth factor-β. *Am J Pathol*. 1994;144:286–295.
30. Tanaka Y, Schuster DP, Davis EC, Patterson GA, Botney MD. The role of vascular injury and hemodynamics in rat pulmonary artery remodeling. *J Clin Invest*. 1996;98:434–442.
31. El-Haroun H, Bradbury D, Clayton A, Knox AJ. Interleukin-1β, transforming growth factor-β_1, and bradykinin attenuate cyclic AMP production by human pulmonary artery smooth muscle cells in response to prostacyclin analogues and prostaglandin E2 by cyclooxygenase-2 induction and downregulation of adenylyl cyclase isoforms 1, 2, and 4. *Circ Res*. 2004;94:353–361.
32. Suzuki C, Takahashi M, Morimoto H, Izawa A, Ise H, Hongo M, Hoshikawa Y, Ito T, Miyashita H, Kobayashi E, Shimada K, Ikeda U. Mycophenolate mofetil attenuates pulmonary arterial hypertension in rats. *Biochem Biophys Res Commun*. 2006;349:781–788.
33. Minamino T, Christou H, Hsieh CM, Liu Y, Dhawan V, Abraham NG, Perrella MA, Mitsialis SA, Kourembanas S. Targeted expression of heme oxygenase-1 prevents the pulmonary inflammatory and vascular responses to hypoxia. *Proc Natl Acad Sci U S A*. 2001;98:8798–8803.

Adenoassociated Virus–Mediated Prostacyclin Synthase Expression Prevents Pulmonary Arterial Hypertension in Rats

Takayuki Ito, Takashi Okada, Jun Mimuro, Hiroshi Miyashita, Ryosuke Uchibori, Masashi Urabe, Hiroaki Mizukami, Akihiro Kume, Masafumi Takahashi, Uichi Ikeda, Yoichi Sakata, Kazuyuki Shimada, Keiya Ozawa

Abstract—Prostacyclin synthase (PGIS) is the final committed enzyme in the metabolic pathway of prostacyclin production. The therapeutic option of intravenous prostacyclin infusion in patients with pulmonary arterial hypertension is limited by the short half-life of the drug and life-threatening catheter-related complications. To develop a better delivery system for prostacyclin, we examined the feasibility of intramuscular injection of an adenoassociated virus (AAV) vector expressing PGIS for preventing monocrotaline-induced pulmonary arterial hypertension in rats. We developed an AAV serotype 1–based vector carrying a human PGIS gene (AAV-PGIS). AAV-PGIS or the control AAV vector expressing enhanced green fluorescent protein was injected into the anterior tibial muscles of 3-week–old male Wistar rats; this was followed by the monocrotaline administration at 7 weeks. Eight weeks after injecting the vector, the plasma levels of 6-keto-prostaglandin $F_{1\alpha}$ increased in a vector dose-dependent manner. At this time point, the PGIS transduction (1×10^{10} genome copies per body) significantly decreased mean pulmonary arterial pressure (33.9 ± 2.4 versus 46.1 ± 3.0 mm Hg; $P<0.05$), pulmonary vascular resistance (0.26 ± 0.03 versus 0.41 ± 0.03 mm Hg $\cdot$ mL^{-1} $\cdot$ min^{-1} $\cdot$ kg^{-1}; $P<0.05$), and medial thickness of the peripheral pulmonary artery ($14.6\pm1.5\%$ versus $23.5\pm0.5\%$; $P<0.01$) as compared with the controls. Furthermore, the PGIS-transduced rats demonstrated significantly improved survival rates as compared with the controls (100% versus 50%; $P<0.05$) at 8 weeks postmonocrotaline administration. An intramuscular injection of AAV-PGIS prevents monocrotaline-pulmonary arterial hypertension in rats and provides a new therapeutic alternative for preventing pulmonary arterial hypertension in humans. (***Hypertension.*** **2007;50:531-536.)**

Key Words: hypertension ■ pulmonary ■ gene therapy ■ remodeling ■ prostacyclin synthase

Pulmonary arterial hypertension (PAH) is an intractable disease that leads to increased pulmonary arterial pressure, progressive right heart failure, and premature death; however, no satisfactory treatment has been established for PAH.[1] Although intravenous prostacyclin (PGI_2) therapy prolongs survival in patients with PAH, the use of this treatment option is limited by the short half-life of the drug, requirement for a continuous infusion system, and catheter-related complications.[1,2] PGI_2 synthase (PGIS) is the final committed enzyme in the metabolic pathway of PGI_2 production. PGIS gene transfer is a promising approach for the stable production of endogenous PGI_2.[3–6] However, previous strategies have several limitations both in the selection of delivery routes and in the efficiency of gene expression. For instance, intratracheal gene transfer may deteriorate respiratory function in critically ill subjects, and the intrahepatic approach may cause peritonitis as a result of direct liver puncture. Although an intramuscular approach seems to be safer than the previous approaches, the conventional plasmid-based strategies achieved only transient gene expression and required repeated gene transfer to inhibit pathological remodeling of the pulmonary artery (PA).[6]

In this study, we used an adenoassociated virus (AAV) vector together with an intramuscular approach to obtain more efficient PGI_2 expression. AAV vectors permit efficient and sustained gene expression in nondividing skeletal muscle cells with minimal inflammatory and immune responses. We reported previously that a stable serum concentration of a secretory protein was achieved over a 1-year period by using a single intramuscular injection of several AAV vector (AAV2 and AAV5) serotypes in mice.[7] Currently, AAV1 is one of the most efficient serotypes for muscle transduction.[8,9]

Received March 25, 2007; first decision April 13, 2007; revision accepted June 22, 2007.

From the Divisions of Genetic Therapeutics (T.I., R.U., M.U., H.M., A.K., K.O.), Cardiovascular Medicine (T.I., H.M., K.S.), and Cell and Molecular Medicine (J.M., Y.S.), Jichi Medical University, Tochigi, Japan; the Department of Molecular Therapy (T.O.), National Institute of Neuroscience, National Center of Neurology and Psychiatry, Tokyo, Japan; and the Department of Organ Regeneration (M.T., U.I.), Shinshu University Graduate School of Medicine, Matsumoto, Japan.

Correspondence to Takayuki Ito or Keiya Ozawa, Division of Genetic Therapeutics, Jichi Medical University, 3311-1 Yakushiji, Shimotsuke, Tochigi 329-0498, Japan. E-mail titou@jichi.ac.jp or kozawa@jichi.ac.jp

Hypertension **is available at http://hyper.ahajournals.org** **DOI: 10.1161/HYPERTENSIONAHA.107.091348**